An Investigation into Adhesive Wear.

A thesis Submitted

in Partial Fulfillment of the Requirements

for the Degree of

Master of Technology

by

Anand Prabhakar Desai

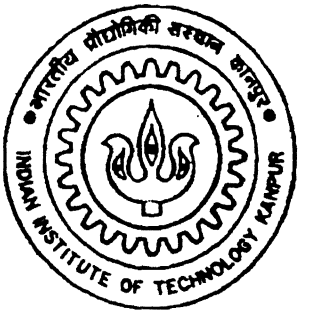

to the

DEPARTMENT OF MECHANICAL ENGINEERING

INDIAN INSTITUTE OF TECHNOLOGY KANPUR

February, 1999

CERTIFICATE

It is certified that the work contained in the thesis entitled **An Investigation into Adhesive Wear** by **Anand Prabhakar Desai**, has been carried out under our supervision and this work has not been submitted elsewhere for a degree.

Dr. M.K. Muju,
Professor,
Department of Mechanical Engineering,
Indian Institute of Technology,
Kanpur. 208016.
February, 1999.

Dr. N.N. Kishore,
Professor,
Department of Mechanical Engineering,
Indian Institute of Technology,
Kanpur. 208016.
February, 1999.

Acknowledgement

I express my sincere thanks to my thesis supervisors Dr. M. K. Muju and Dr. N. N. Kishore for excellent guidance, constructive advice, constant support and encouragement throughout the present work.

Many special thanks to Mr. R. M. Jha, Mr. H. P. Sharma, Mr. Namdeo and MR. Anil for their help during experimentation.

A special word of thanks to Dr. Dixit and Dr. Prashant Kumar for giving me permission to do work in their laboratories.

Finally I express thanks to all my friends and classmates for making my stay at I.I.T. Kanpur a memorable one.

Anand Prabhakar Desai.

Dedicated

to

Sachin Gajare

Abstract

A welded asperity junction is formed during rubbing motion between two surfaces, wherein the asperities come into contact to form welded junctions under intense local stresses. The fracture takes place at the junction as result of motion of one of the surfaces. A loose wear particle get formed after a large number of such interactions occur. The wear coefficient defined in literature is based on this loose material. The junction formation is of two types, unimetallic and bimetallic. Unimetallic junctions are formed during sliding of similar metals, while bimetallic junctions are formed during sliding of dissimilar metals. In the present work, finite element technique is used to examine the fracture path during relative sliding of a single asperity junction. An attempt is then made to calculate wear coefficient with the help of fracture path in unimetallic and bimetallic junctions using Brockley and Fleming's model. This is defined here as adhesive wear coefficient. The model taken is a symmetrical junction. Finite element technique is applied to both types of junctions, unimetallic and bimetallic. A package, CSA-NASTRAN is used for finite element analysis. An experimental work is also carried out on copper, mild steel and lead to get qualitative agreement on crack initiation. Experimental results show that the crack initiates and propogates into both the asperities for an unimetallic junction. The fracture path at an asperity junction shows qualitative similarity to that of Brockley and Fleming's results. The results show that the adhesive wear coefficient is higher for unimetallic junctions than for bimetallic junctions. This shows that for higher compatibility metals, wear coefficient is more, in turn more wear. An attempt is made to compare the adhesive wear coefficient to the wear coefficient available in the literature. The results have shown that adhesive wear coefficient increases as the ratio of Elastic modulus to the Hardness of softer material in the junction increases. The adhesive wear coefficient gives similar trend to the wear coefficient (defined using Archard's equation) when plotted against ratio of Elastic modulus to Hardness of softer material in the junction.

Contents

List of Figures

List of Tables

Chapter 1

Introduction

Although the laws of friction are fairly well substantiated, there are no satisfactory quantitative laws of wear. In general it is safe to say that wear increases with time of running and that with hard surfaces the wear is less than with soft surfaces. But there are many exceptions and dependence of wear on load, nominal area of contact, speed, hardness etc., is even less generally agreed upon. This is because there are many factors involved in wear and slight changes in conditions may completely alter the importance of individual factors or change their mode of interaction. In short, there is no sound law of wear by which we can predict the wear.

Under the action of frictional forces, contacting asperities can be destroyed in a number of ways. The type of destruction depends on both the properties of rubbing materials and on the external conditions such as load and speed.

Classification of wear mechanisms was proposed [1] in following manner.

- Adhesion or Galling
- Abrasive
- Diffusion
- Corrosion
- Thermal wear.

It is clear from several experiments [1] that the interacting surfaces make contact only at a few isolated points, resulting in high stresses in those areas. This gives rise to plastic flow at the interface. The resistance to sliding is equivalent to the sum of the shearing forces necessary to break up all these junctions. When laws of wear were tried to formulate, much attention has been paid to adhesive wear which can be defined as being that process which gives rise to loss of metal between interacting surfaces as a result of adhesion of asperities.

1.1 Literature Survey

The surfaces of solids are wavy and rough. Even the smoothest metallic surfaces have irregularities of about 0.05-0.1μm [2]. Manufacturing inaccuracies in components, distortion of their shape due to stress, temperature, the roughness and waviness of surfaces all result in materials contacting each other only over small discrete areas. Because of waviness, these areas are located in well defined regions. The number of contacts depends upon both the load and roughness of the surface. Thus the real contact area is less than apperant contact area.

It is generally agreed that when two surfaces are pressed together either statically or in sliding contact real contact occurs at the tips of asperities, where plastic deformation takes place under intense local stresses. The work of deforming the asperities in sliding gives frictional forces and the deformation itself leads to wear and to metal transfer between the surfaces.

With respect to dry wear, several theories have been proposed. Holm [3] developed a wear equation which was based on encounters between individual atoms. Holm reached the following conclusions,

- The real area of contact is formed by plastic deformation of contacting asperities and
- Wear is caused by atomic interaction between the two surfaces.

According to Holm,

$$W = \frac{ZP}{H} \tag{1.1}$$

Where,

W= Quantity of wear debris produced per unit distance of sliding.

P= Load.

H= Hardness.

Z= Probability of removal of an atom from the surface, when it encounters another atom or in other words, the number of atoms which are removed on encountering all the other atoms within a unit area per unit distance of sliding.

Archard [4] also gives the primary equation of wear.

$$\frac{V}{L} = Z\frac{N}{P_m} \tag{1.2}$$

Where,

Z = Coefficient of wear.

N = Load.

L = Sliding Distance.

P_m = Flow pressure of material.

The wear consists of different processes. The wear coefficient for different processes lies in different range. Fig. 1.1 shows the range of wear coefficient for different wear processes for metal. Fig. 1.2 shows the same for ceramic [5]. It is clear that for harder surface e.g. ceramics, adhesive wear coefficient is low compared to soft metals.

Wear can be classified in a variety of ways, but none has yet proved to be completely satisfactory. It is now becoming evident that a clear distinction must be made between the different processes responsible for detaching particles from a surface and those involved

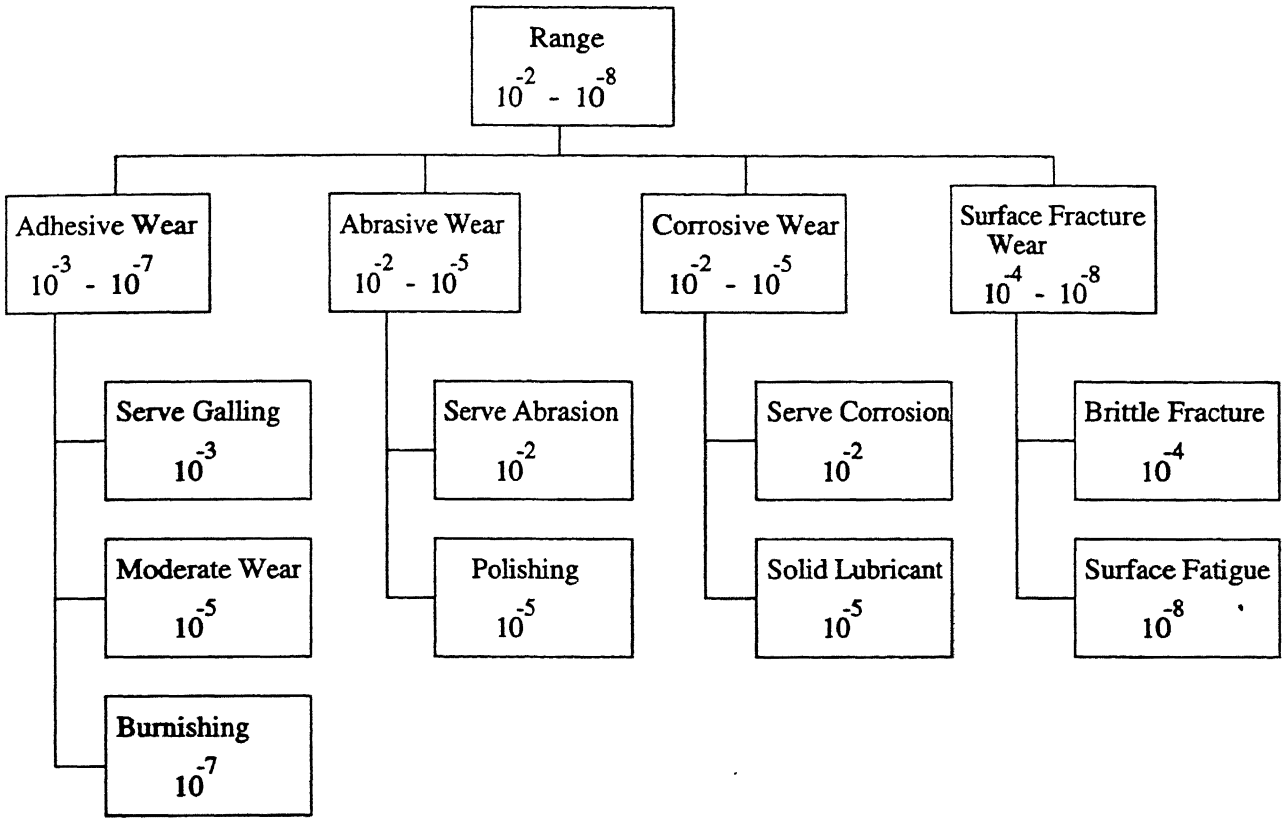

Figure 1.1: Typical Wear Coefficient values for Metal-on-Metal Sliding Systems.

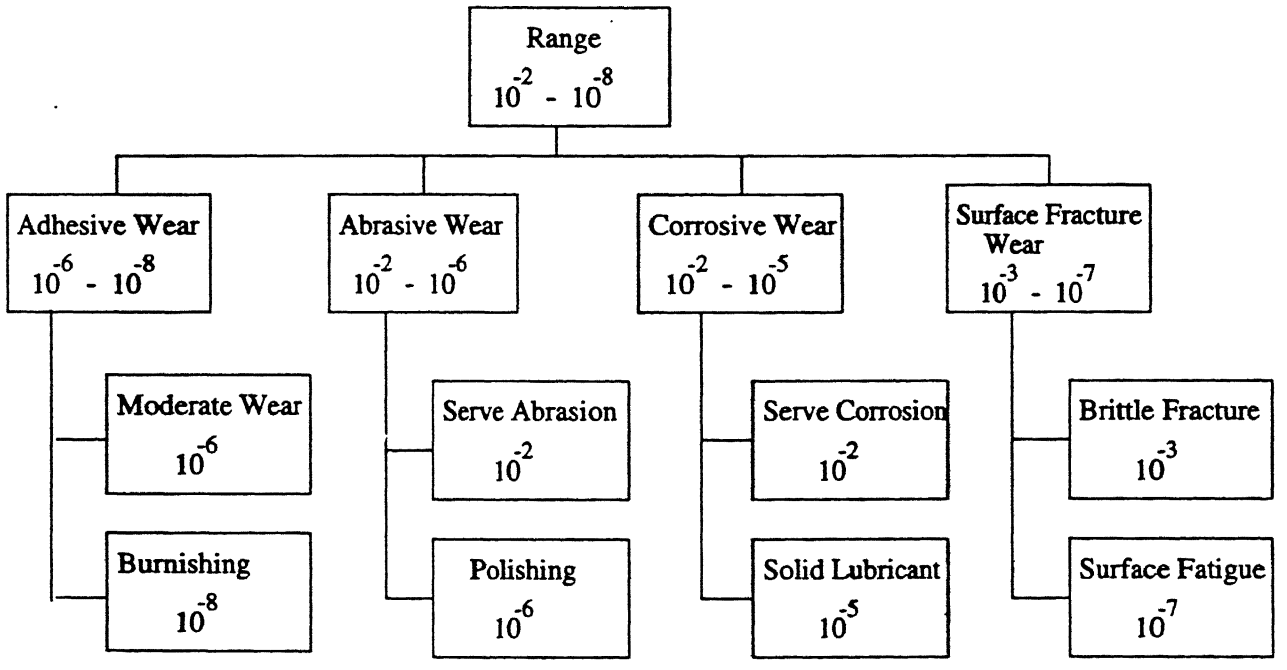

Figure 1.2: Typical Wear Coefficient values for Ceramic-on-Ceramic Sliding Systems.

in the production of debris. Particle production via crack propagation appears to be a common feature with many materials, but appropriate models still await development.

The tendency of the contacting surfaces to adhere arises from the attractive forces which exist between the surface atoms of the two materials. If two surfaces are brought together and then separated, either normally or tangentially, the attractive forces act in such a way as to attempt to pull material from one surface to the other. Whenever the material is removed from its original surface, an adhesive wear fragment is created. The strength of bonding at the points of adhesion is sometimes so great that while attempting to free the surface, separation takes place not along the interface but in one of the bodies itself resulting in metal transfer and subsequent metal removal. This will occur if the force is greater than the required to break through some continuous surface inside one of the materials. It has been experimentally observed [6] that because of the intense local stresses at the junction, strong adhesion generally occurs at the interface and hence fracture takes place mostly along some path inside one of the materials. Thus under some conditions, loss of material may occur from one or from both of the rubbing pair. This type of wear is called as adhesive wear. This is the most common form of metal wear and exists predominantly at moderate cutting conditions. The removal of material takes place in the form of small particles which are generally transferred to the other surface, but may also come of in loose form.

Almost all wear processes adhesive wear is the process which is mostly found out. In adhesive wear mainly following stages happens [7].

1. Matching up of two asperities.
2. Adhesion of these asperities across the interfade.
3. Fracture initiation at a critical point.
4. Transfer of material from one asperity to another.
5. Subsequent disintegration and removal of this transferred material

1.1.1 Junction Formation between contacting bodies.

A closure examination of these discrete regions of contact has revealed further that the actual contact between between bodies occur at certain high points located within these

regions. These regions are called as contact points or more commonly asperities. Problems connected with metal transfer and wear during sliding process are very much dependent on the nature of phenomenon taking place at these contact asperities. These asperities are subjected to extremely high stresses even at ordinary loads, because of their small dimensions. Due to the high stresses, contact of the two bodies at the asperities generally results in formation of junctions which have been the subject of investigation for many research workers.

A widely held ideas of Bowden and Tabour [8] on the nature of wear are based on a picture of the formation of welded junctions and their subsequent destruction.

The exact mechanics of particle formation for wear are of interest. A detailed study of the microscopic events involved in the interaction between actual surface asperities posses a number of problems. However the junction model Green [9] offers a possible method for experimental investigation of wear particle and formation at a greatly magnified scale Fig 1.4.

Green [6] assumed that asperities approach one another and weld together during relative parallel sliding of surfaces. He replaced the random geometry of the actual surface by an idealized configuration which permitted theoretical solution for the force relationships established during the shearing of the junctions. Green imposed two conditions in his theoretical study namely,

1. No normal motion takes place between opposing surfaces.
2. contacting asperities have strong adhesion.

In this theoretical analysis, Green [6] derived a plain-strain solution for thick junctions and a plane-stress solution for thick junctions and a plane-stress solution for thin junctions.

In a Paper by Green [9], asperity was modelled as shown in fig 1.3. At any instant when the junction is formed, Force acting through the junction has a normal component N_1(compressive) and tangential component F_1 (shear) as shown in fig. 1.3. Rough estimations of the forces exerted through such models have also been attempted by Edward and Halling [10] and Gupta, Cook [11].

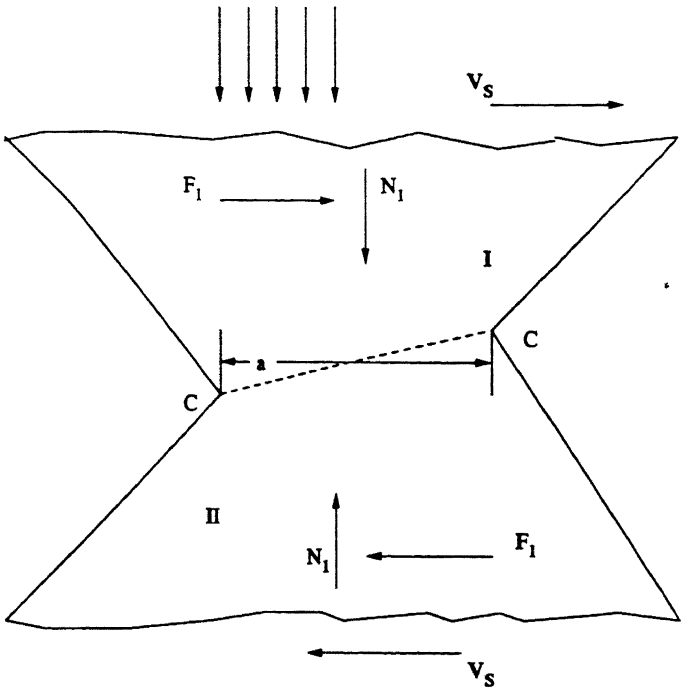

Figure 1.3: Model of an asperity junction.

We consider the asperities just have met as in fig. 1.5(a). A mean normal stress (compressive) P_1 and tangential (shear) stress S_1 act through the junction. Due to these stresses the junction is deformed so that the two surfaces move parallel to one another. These stresses calculated by Green [9] are shown in fig. 1.6. For normal values of surface roughness, angles δ_1 and θ_1 are less than 10°. When a junction is formed, for such values of δ_1 and θ_1, it can be seen from fig 1.6 that $S_1 \cong 1.25\,K_1$ and $P_1 \cong 2\,K_1$ where K_1 represents the yield stress in shear of the softer body. Further deformation is as shown in fig. 1.5(c) and fig. 1.5(d), causes changes of shape such that θ_1 increases and δ_1 decreases. It is also seen from fig. 1.6 that δ_1 decreases and θ_1 increases. S_1 tends to become K_1 and P_1 decreases continuously. Also as the junction tends to become roughly symmetrical P_1 continues to decrease. Thus where junction has been deformed to the symmetrical shape, the normal stress on it is zero and the tangential stress is nearly equal to its initial value. After the symmetrical shape has been achieved, the cycle gets reversed (Fig. 1.7.) i.e. S_1 increases slightly while P_1 becomes tensile and remains so until the junction eventually breaks under combined shearing and tensile forces. Thus the asperities have matched up and firmly welded the cross-section 'a' remains approximately constant until necking and fracture commences.

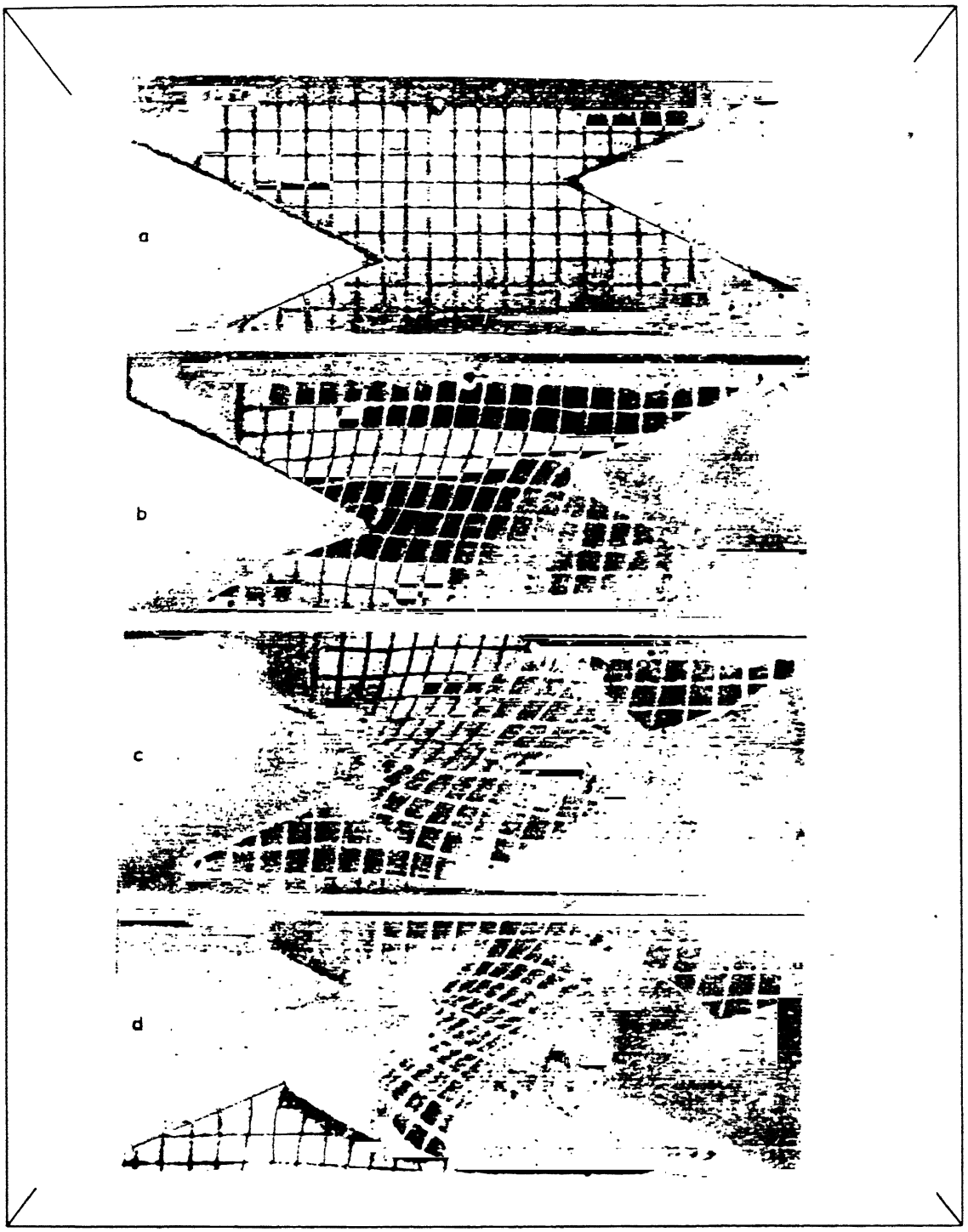

Figure 1.4: Crack path in a unimetallic junction.

1.1.2 Transfer of Material

It has been proved that a crack propagates at an adhesive junction and fracture ocurrs at the junction giving the wear particle or material may be transfered from one asperity to the another.

The direction of material transfer may be classified in 3 ways. One way transfer (A→B or B→A), mutual transfer (A→B and B→A) or back transfer (A→B→A etc.). Evidence for all three has been claimed in the literature [12], but as yet there is no reliable theory to predict the direction and relative amount of transfer for a given system. The simplest theory states that transfer should occur if the shear strength of adhesive bond between two asperities is greater than that of transferring material. Thus one might expect the "softer" material to transfer to "harder" material. But this rate is not always obeyed. One complicating factor is the test geometry. It is known that the dominant direction of transfer may depend on the geometry of sliding system. For a pin on disk system, transfer is preferentially from the disk to pin, unless the unworn flat is much harder than the unworn pin. Sreenath and Raman [13] observed that the loose particles resulting from wear may fill valleys.

From the fundamental view point, adhesive wear must be related to the cohesive strengths of the two counterfaces and the adhesive strength of interface. Based on the cohesive energies of the metals involved, Buckley [14] was able to predict that the direction of the material transfer would be from the cohesively weaker to the cohesively stronger material.

1.1.3 Adhesive Wear

Due to fracture at adhesive junction a fragment of one asperity is transfered to the other. The transfer fragments gradually increase in size until the mechanical stresses which they suffer become sufficient to detach them as loose wear particles.

There are various experiments carried out to find out the wear between different combination of metals [15,16,8]. With repeated traversal of the same region, the transferred fragments accumulate and lead to the formation of wear debris. Using a radioactive pin of

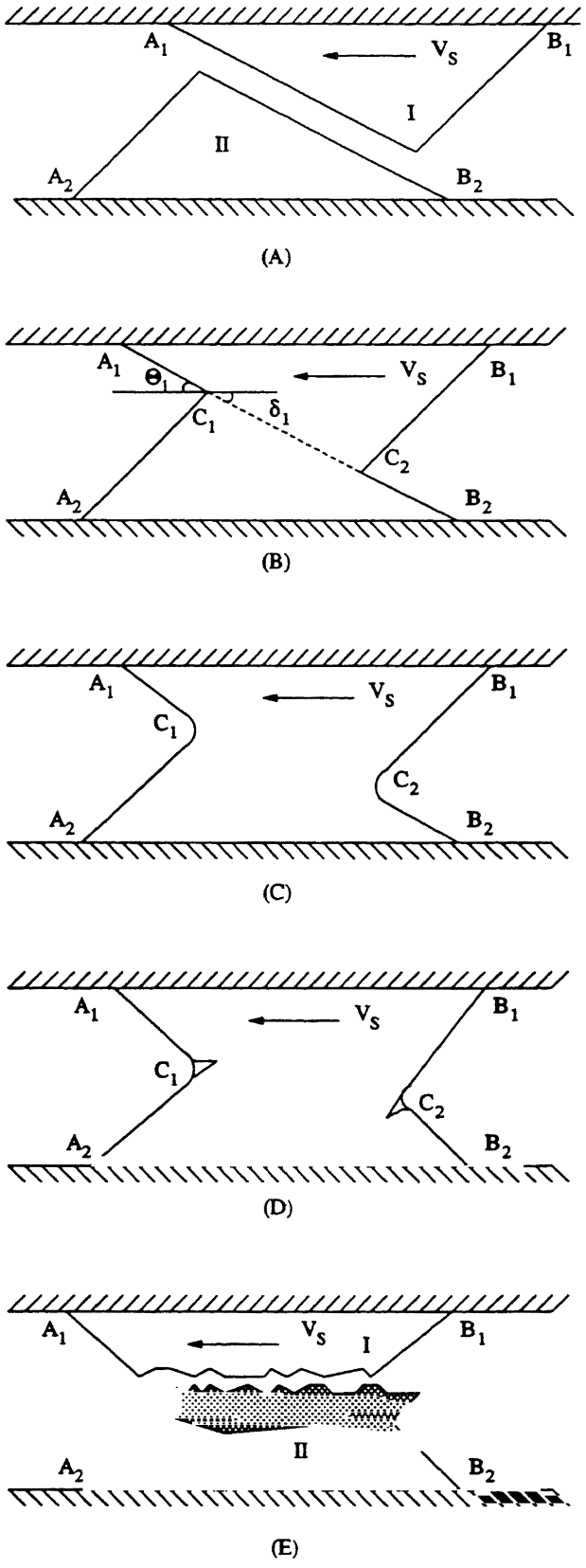

Figure 1.5: Fracture of a asperity junction

60:40 leaded brass rubbing on a tool -steel ring, Kerridge and Lancaster [17] have studied both processes. The amount of debris steadily increases with the time of sliding, but the amount of metal transfered and adhering to ring soon reaches equilibrium.

The wear debris have different shapes like plate, ribbon, cylinders, spheres, cutting chips, irregular chunks and loose clusters [12].

The high wear rates occurring in serve wear is due to primarily to the shearing of intermetallic junctions and constitutes the simplest type of wear processes. If we consider behavior of relatively clean metals under high specific loading, we may envisage four different situations.

1. The interface is slightly weaker than either of two sliding metals, shearing will then occur in the interface itself and the wear will be small. e.g. tin on steel.
2. The interface is stronger than one metal but weaker than other. The shearing occurs in the softer metal and fragments of this are left adhering to harder surface e.g. lead on steel.
3. The interface is stronger than one metal and occasionly stronger than other. There is marked transfer of softer on harder but occasionly harder metal also plutched out. e.g. copper on steel.
4. The interface is always stronger than both metals and shearing takes place at a short distance from the interface. This occurs in sliding of identical metals and result in damage of both surfaces.

The way in which wear particles form is graphically illustrated by experiments of Green [9] who used two dimensional models of various metals and plasticine to denote asperities and then sheared the asperities.

The stages through which junction have been observed to be passing can be understand with the aid of fig. 1.5. The figure illustrates the deformation of asperities I and II of similar hardness. After the initial adhesion most of the center of the junction is sheared uniformly, fig. 1.5(c). Due to this shearing the interface gets stretched. This would help to break any surface films present and thereby strengthen the adhesion. As the tendency

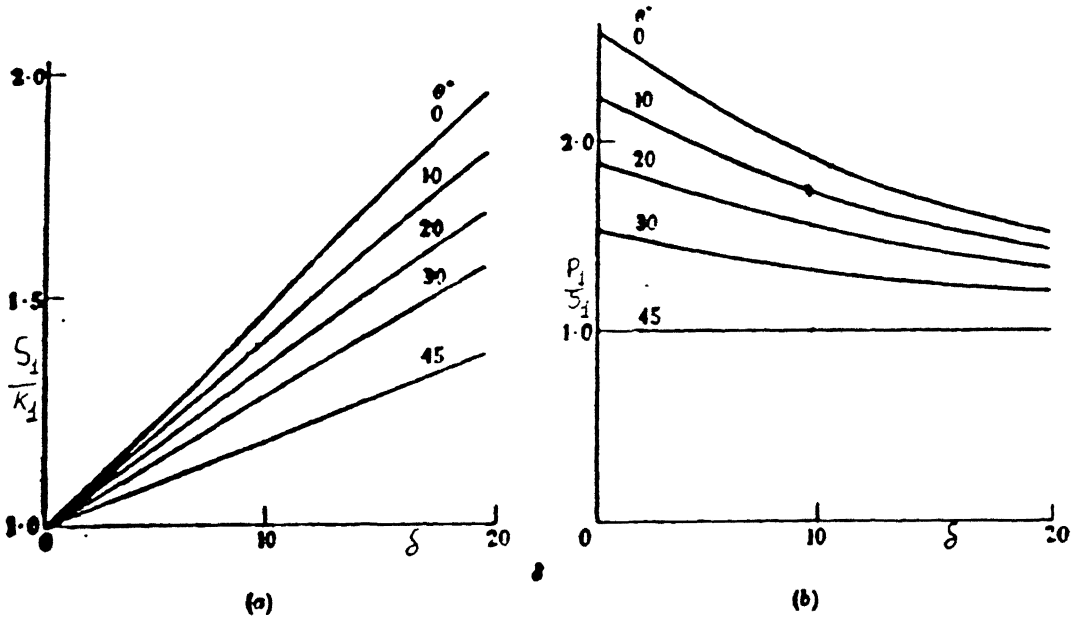

Figure 1.6: Theoretical relations for strong junction.

for the asperities to pass each other continues an intermediate stage shown in fig. 1.5(d) is reached when the junction has acquired a symmetric shape. Since the adhesion is assumed to be fairly strong the junction deforms as a single body and thus necking and fracture occurs in the most critically stressed region of the junction. In this manner a small particle is transferred from one asperity to the other one. In a subsequent encounter this transferreed material may become a loose wear fragment.

Experiments have shown that most of the times the softer asperity looses material to the harder one, but the probability of the harder body loosing material is also finite. The reason for this is the presence of weak spots within the harder asperity as well as its fatigue caused by the interactions. In general, therefore, the fracture occurs more often on the side of the softer asperity as against that of the harder asperity.

Brockley and Fleming [18] conducted the experiments on copper metallic junctions cut from one piece. these single piece junctions were made to shear by applying a load from a motor. They studied the failure of these junctions is shown in fig. 1.4. The figure illustrates that junction formed by two identical materials has equal probability of failure on either side of the interface. This figure also indicates that compression, rotation, tension and shearing at the ends of the junctions are apparently involved in the process. Thus the mechanism of wear fragment formation is quite complex and does not render itself to convenient analytical solution. However rough estimates of the forces exerted through

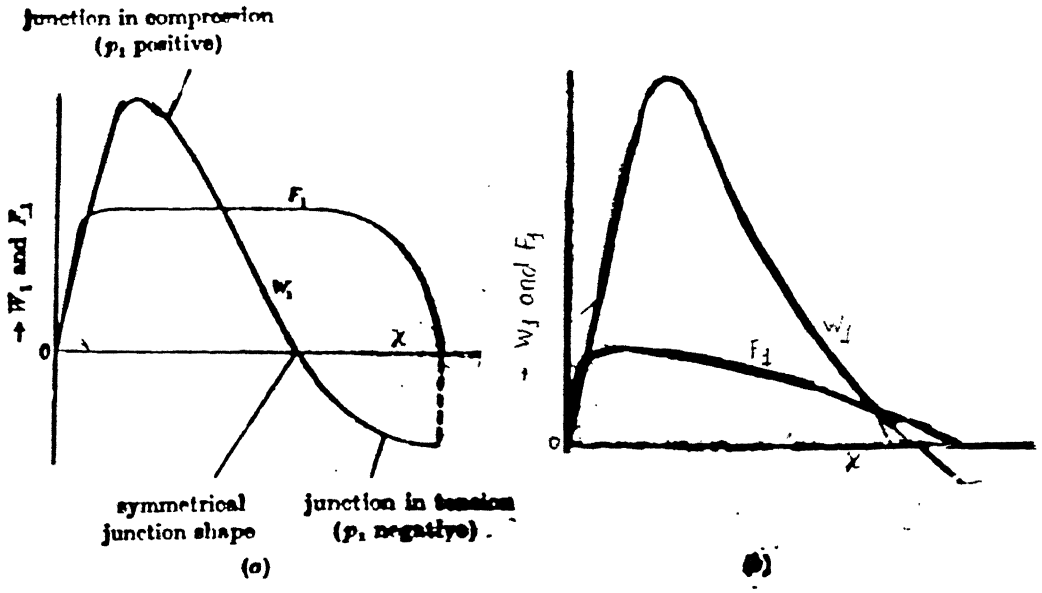

Figure 1.7: Theoretical estimation of the relation between the forces exerted on a junction and the relative displacement of surfaces (qualitative only).

such junctions have been attempted by Green [9], Edward and Halling [10], Gupta and Cook [11].

Baliga [19] tried to predict the path of a crack through unimetallic junctions. He took brittle and ductile materials for his model. Baliga stated that the crack starts at the interface and goes into one of the asperity.

1.1.4 Factors Affecting Adhesive Wear

Archard's equation shows that the wear depends on load, hardness etc., but there are many other variables which control the adhesive wear. These variables are 1) Compatibility 2) Ratio of Elastic modulus to the hardness 3) Adhesion energy ratio, R.

An increase in the magnitude of friction and wear is experienced when materials slide in high vacuum. The reason for this high friction is attributed to the formation of strong junctions which grow and cohere due to solid phase welding of the asperities. Diminished junction growth and hence score or wear resistance of metals has been correlated with the solid solubilities of metal combinations clearly, albeit in a qualitative way [20] e.g. lead, tin and indium have very limited solubility in iron and a combination of these elements with iron provides the basis for a good bearing situation. On the other hand, very poor

score resistance (i.e. high adhesive wear) is experienced with a combination of iron and nickel which have very large mutual solid solubility.

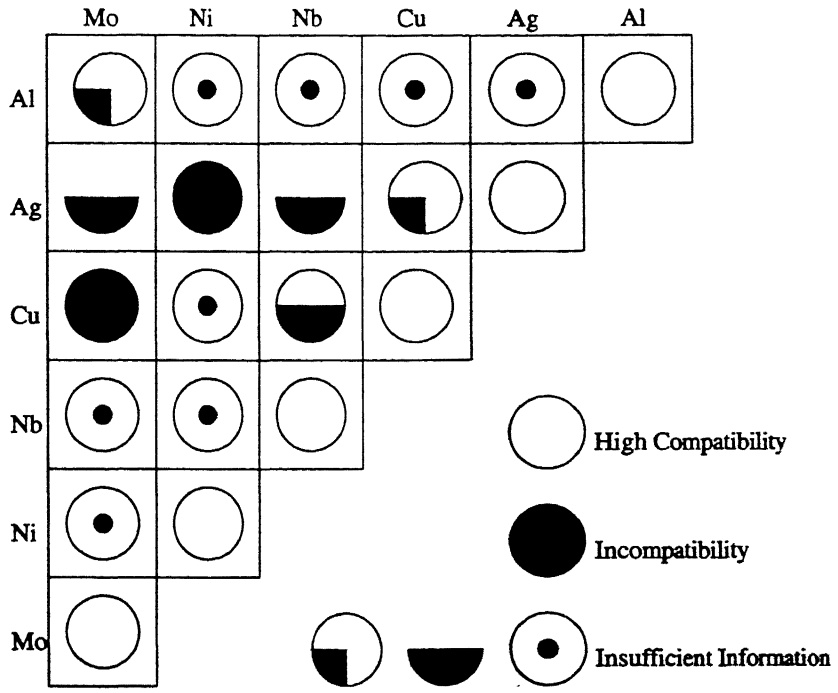

Figure 1.8: Compatibility for metals

Some researchers [21] carried out experiments with different metals and iron. They found score resistance of materials according to the classification was as follows.

- Very Poor : Beryllium, Nickel, Titanium, Iron, Cobalt, Gold etc.
- Poor : Magnesium, Aluminium, Zinc, Tungsten etc.
- Fair : Carbon, Copper, Aluminium etc.
- Good : Indiumcircles, Silver, Tin, Lead, Bismuth etc.

It is clear that when there is poor score resistance, adhesion will be high and for good score resistance adhesion will be very low.

It is seen from these results that the materials which have good resistance to surface damage have either a limited solubility in iron or form intermetallic compounds with

it. These experiments suggest that contact between surface without contaminants is important, if the fundamentals of metallic interaction is to be understood.

Rabinowicz [22] showed that wear coefficient depends on the ratio of the interfacial surface energy of adhesion to the sum of the surface energies of the contacting surfaces. The calculations of the energies involved in wear particle production [23], which indicate that wear particles that can come off a surface by an adhesive wear processes must have a characteristic particle, the least diameter d_A of a particle formed by the one time rupturing of an adhesive bond must have the value given by equation.

$$d_A = \frac{60000 W_{ab}}{P} \tag{1.3}$$

W_{ab}= surface energy of adhesion at the interface and P is the hardness of material being worn.

It had been shown that for cubic structured metals, one promising parameter is ratio $\frac{W_{ab}}{(\gamma_a+\gamma_b)}$ and is between zero and one. The experiments [22] were carried out and found the compatibility relationships for metals. Fig 1.8 shows compatibility relationships for six metals. Black circles denotes incompatibility, open circles full compatibility, while others are intermidiate. The two half circles denotes insufficient information based on the binary phase diagram. It can be argued that, high compatibility would mean high interfacial surface energy.

Fig. 1.9 shows variation of wear coefficient as a function of surface energy ratio, R. It is observed that for high compatibility, R have higher value. High R would lead to high adhesion and high friction. It had been found that wear coefficient varies square of R. Similar figures are available for wear coefficient against surface roughness and friction coefficient. There is tendency for the compatible and incompatible points to lie on different lines. Thus compatibility plays major role in the adhesion.

It has also been shown that adhesive bonding between materials is related to their modulus of elasticity and hardness. Halling and El. [24] has discussed the plasticity index ψ which essentially depends on the ratio of $\frac{E}{H}$,

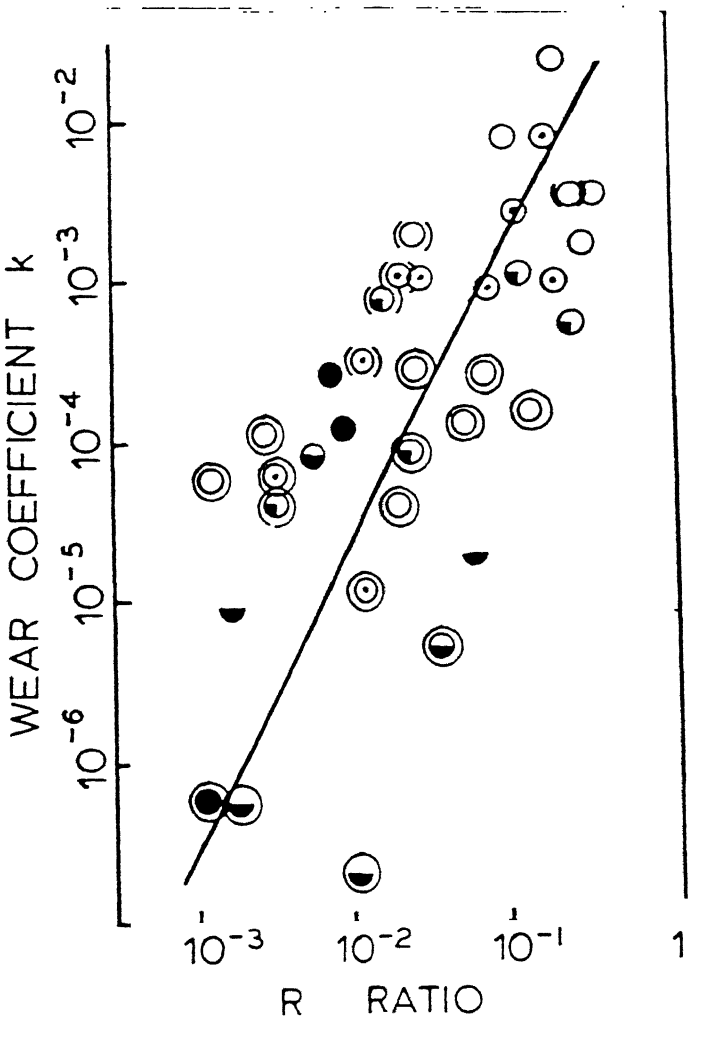

Figure 1.9: Wear coefficient Vs Surface energy ratio,R

$$\psi = \frac{E}{H} n \sin\theta \tag{1.4}$$

where

E = elastic modulus of elasticity of the material

H = hardness of the material

θ = base angle of an asperity

n ≈1.7-2.4

Authors had shown that for $\psi > 1$. conditions are plastic at interface, while for $\psi <$ 0.6, conditions are elastic. As plasticity index increases the plastic deformation at the interface increases. The friction and wear assume plastic condition of the sliding interface. Examinations show that the interface work hardens to a finite depth. If the surface is hard, further plastic flow should not be expected. This plasticity index value is important quantity predicting the contact of nature and in turn wear, thus suggesting that $\frac{E}{H}$ is a factor affecting wear.

1.2 Objective and Scope of the thesis

In this present work an attempt has been made to examine how the junction fracture proceeds as sliding of one asperity over another continues and whether this could be used to compare the wear coefficient for different material combinations. The adhesion wear coefficient, K was obtained with the help of model defined by Brockley and Fleming [18] based on the assumption that every asperity junction produces a wear particle. The volume of wear was calculated with the help of the path of fracture at welded asperity junction formed during adhesion of two asperities in sliding contact. The path has been obtained using finite element analysis.

The present work is basically divided in two stages. The path of fracture for two different kinds of asperity junctions has been studied;

(1) Unimetallic junction wherein fracture takes place in both the asperities.

(2) Bimetallic junction wherein fracture takes place only in one asperity of softer metal.

Unimetallic junction is the junction formed due to sliding of similar metals over each other and bimetallic junction is the junction formed due to sliding of different metals over each other.

The main scope of this work would be to estimate crater wear in cutting tools during machining, where crater wear occurs due to adhesive wear between chip and tool.

Chapter 2 contains a brief description of the finite element method. A brief description of package, CSA-NASTRAN and CSA-GENSA is also given.

Chapter 3 describes the experimentation and problem methodology. It gives how the experimental work is carried out. The model used to calculate the wear coefficient is also explained.

Chapter 4 the results of the experiments and Finite element modeling are given. Some discussion is also carried out. The acceptability of the model proposed is also justified.

Chpter 5 gives conclusion and scope for future work.

Chapter 2

Finite Element Analysis

2.1 Introduction

The FEM's usefullness and its versatility lies in its ability to easily accommodate material nonlinearities, geometric nonlinearities and complex geometries. Chapter briefly outlines the theory of finite element method and its formulation and the procedure of determining the path of crack propagation in the asperity junction. A brief description of packages CSA-NASTRAN is also given.

2.2 The Finite Element Method

Finite Element Method is now very well described in a number of books [25,26]. FEM is a numerical discretisation procedure by the use of which a wide range of complex boundary value problems can be analyzed. The basic concept of FEM is derived from structural analysis. Here every structure is approximated as a physical assemblage of individual structural components or finite elements. The elements are interconnected at a finite number of nodes and sometimes along the boundaries of the element. Assuming the approximate behavior of individual elements, the behavior of the entire system can be analyzed. After assembling the individual elements, the necessary boundary conditions are imposed, with primary nodal values as unknowns. Solution of the resulting set of equations yield the system response.

In matrix form, the system equation can be written as,

$$[K]\,\{u\} = \{Q\} \tag{2.1}$$

in which,

$$Stiffness\,Matrix,\ [K] = \sum_{e=1}^{NEL} K_{ij}^{(e)} \tag{2.2}$$

$$Force\,Vector,\ \{Q\} = \sum_{e=1}^{NEL} Q_i^{(e)} \tag{2.3}$$

and

$$Displacement\,Vector,\ \{u\} = \sum_{e=1}^{NEL} u_i^{(e)} \tag{2.4}$$

The displacements can be expressed as

$$U = \sum N_i\, a_i^e = [N_i\,,\ N_j\,,\ .....] \begin{Bmatrix} a_i \\ a_j \\ . \\ . \\ . \end{Bmatrix}^e = N\, a^e \tag{2.5}$$

where,

U = displacement at any point within the element.

N = prescribed function of position called shape function.

a^e = nodal displacement vector for a particular element.

The strain vector, ϵ, can be obtained with displacements known at all points within the element,

$$\{\epsilon\} = [B]\,\{a\} \tag{2.6}$$

[B] is strain-displacement matrix.

For a linearly elastic constitutive law stress can be obtained as,

$$\{\sigma\} = [D]\{(\epsilon - \epsilon_o)\} + \{\sigma_o\} \tag{2.7}$$

where,

$\{\epsilon_o\}$ = initial strain matrix.

$[D]$ = stress strain matrix.

$\{\sigma_o\}$ = initial residual stresses.

Following the virtual work principle or minimum potential energy principle, it can be shown,

$$[K_e] = \int_{A^{(e)}} B^T D B \, t \, dA$$

2.3 Crack Propagation and Simulation

When two metals are sliding, the asperities are under normal load (N) as well as tangential load (S) (Fig. 2.1(a)). Because of these loads, the asperities adhere to each other (Fig. 2.1(b)). It had been experimentally observed [6,11] that the junction becomes symmetrical about the interface (Fig. 2.1(d)). The junction starts fracturing as shown in fig. 2.1(d). Green [9] showed that the junction experiences compressive load first and later it experience tensile load. Thus the crack will not propagate until it is under tensile stress condition. There will be some strain hardening in the junction. In FEM analysis it was assumed that normal load is already applied and junction is on the verge of fracturing.

The process of junction failure was analyzed using the finite element method with the following assumptions.

1. The junction failure is assumed to occur under conditions of plane stress.
2. Large deformation theory is not considered for the analysis.
3. The material is considered isotropic, linearly elastic.

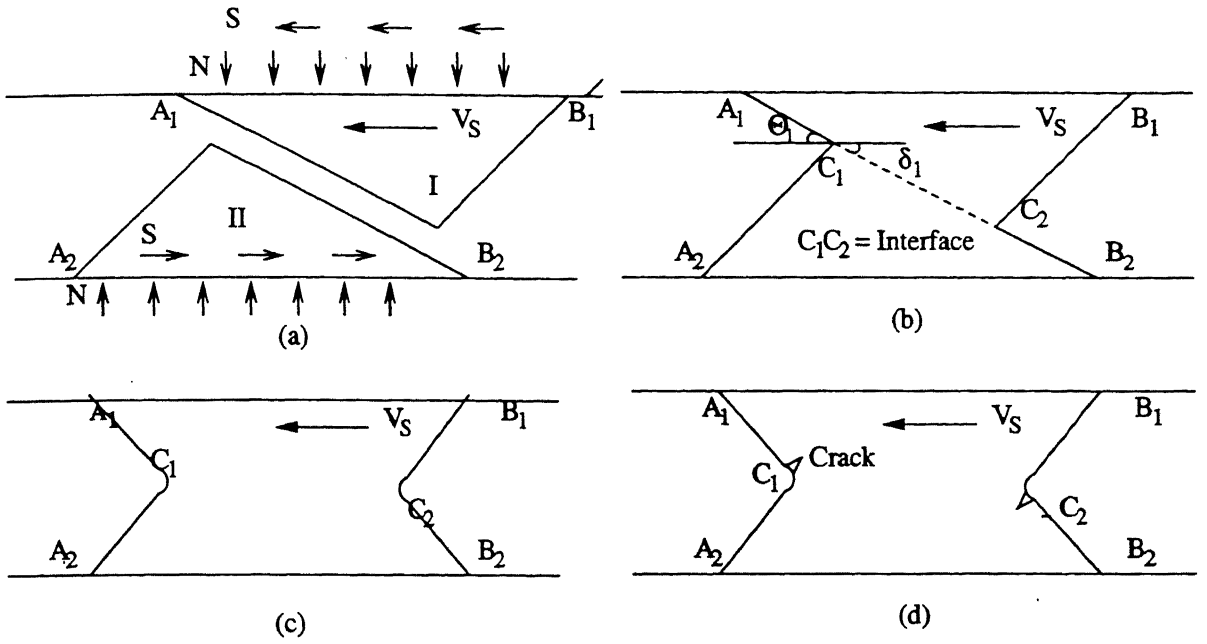

Figure 2.1: Interaction of Asperities.

Small cracks at the asperity junction are assumed (Fig. 2.1(d)). This crack will propagate under strain energy density criteria.

The problem described above was solved using the package CSA-NASTRAN and CSA-GENSA. The asperity junction is discretized as shown in fig. 2.2. The study of wear, involved the modeling of crack propagation usually emanating from the asperity junction. The propagation is simulated by using the concept of double nodes.

The procedure for analysis was as follows.

The geometry was created as shown in fig. 2.2. The geometry used was a symmetrical junction. It was created using FEMAP50 package. The boundary surfaces were defined. Two separate boundary surfaces were defined assuming that there are two asperities. The material was defined using the material library of the package. The materials which were not in the library, were added and saved. Depending upon the junction type, bimetallic or unimetallic, material(s) were defined. The element chosen was in-plane plate element. An isotropic property was chosen. The mesh was created by defining the number of elements on each curve. 3-nodded triangular elements were used for the analysis. The loads were defined on the respective boundaries and then constraints were defined. The load applied

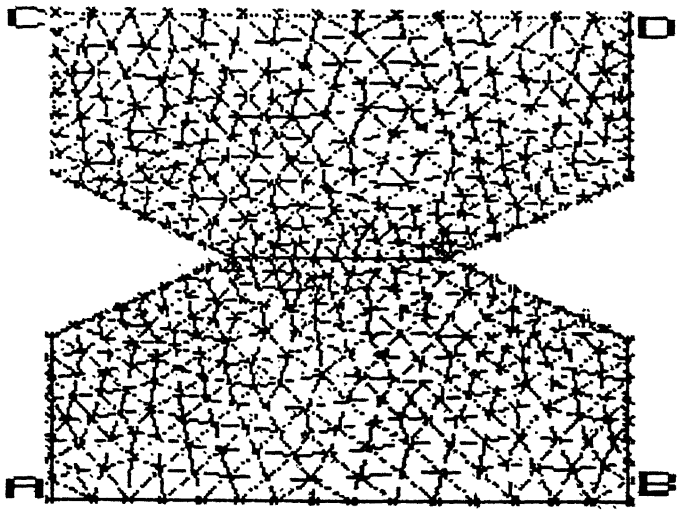

Figure 2.2: Model for FEM.

was equal to the shear strength of the material, as the length of interface was taken as one unit. For bimetallic junction, different properties were used during meshing command. This defines different metals for both asperities. The points, elements, nodes were checked for coincidence. This problem arose mostly for bimetallic junction, as the mesh was defined in several subregions. If coincident points found, they had been merged, so that one single geometry could be created. The whole model was exported to NASTRAN or GENSA depending on the analysis type to be run. If model was exported to GENSA, a file named model-name.nli was created and some necessary cards were inserted. The analysis was run using respective command.

After the analysis is completed, the output file was imported into FEMAP. The stresses, strain energy density at the connecting nodes, elements of the crack were observed. The node coordinates of the node having minimum strain energy density were noted down. The minimum strain energy density criteria was used for finding out the direction of the crack. It was assumed that if the XY shear stress at that node exceeds shear strength of material, the crack will propagate. The XY shear stress of that node was examined for above reason. Then again the same geometry was opened in FEMAP. The crack was made to propagate by creating two nodes at the tip of previous crack and crack was extended to the new point noted down. The remeshing of the geometry was done. The loads and constraints were applied and again the geometry was exported to GENSA and run. This procedure was repeated until crack propageted to the desired length.

2.4 CSA-NASTRAN

In the present work, NASTRAN package is used for the finite element analysis of an asperity junction. CSA-NASTRAN is a very powerful FEM package. It can accommodate many the types of FEM problems along with 2D and 3D elements. CSA-NASTRAN is a basically a package which meant for elastic analysis, while CSA-GENSA is the the package which can analyze the nonlinear problems. FEMAP50 is the preprocessor used for the analysis. It can help the user to input the problem geometry and apply various boundary conditions.

The input file for the NASTRAN is filename.DAT. The same file can be used for input for GENSA with some modifications. Another file named filename.NLI includes some cards essential for nonlinear analysis, such as load increment, material definitions etc.

The results of the analysis can stored in default output files. These results can be imported in FEMAP50 and can be seen graphically. The options available are animation, contour etc.. The values of the output can be seen at required nodes and elements.

Chapter 3

Experimentation and Problem Methodology

3.1 Introduction

This chapter describes the details of actual problem of welded asperity junction, experimentation. The calculation of adhesive wear coefficient is also stated.

3.2 Problem Description

The asperity shape has been modelled as triangular shape by several researchers [9,18]. The Fig. 3.1 shows the junction formation between two asperities having triangular shape.

Fig. 3.1(a) shows two triangular asperities, moving towards each other. Each asperity is experiencing normal load (N) and tangential load (S). Fig. 3.1(c) shows the asperities just have touched each other. Fig 3.1(d) shows that the adhesion is taken place between these two asperities as a result of loads. Thus one gets the shape shown in fig 3.1(d), where dotted line shows the welding at the junction. The result will be the single shape through strong adhesion or welding of two asperities.

Brockley [18] modelled the asperity junction as shown in fig 3.1(d). The shear force was applied to the junction. The junction failure was examined as explained in section 1.1.4.

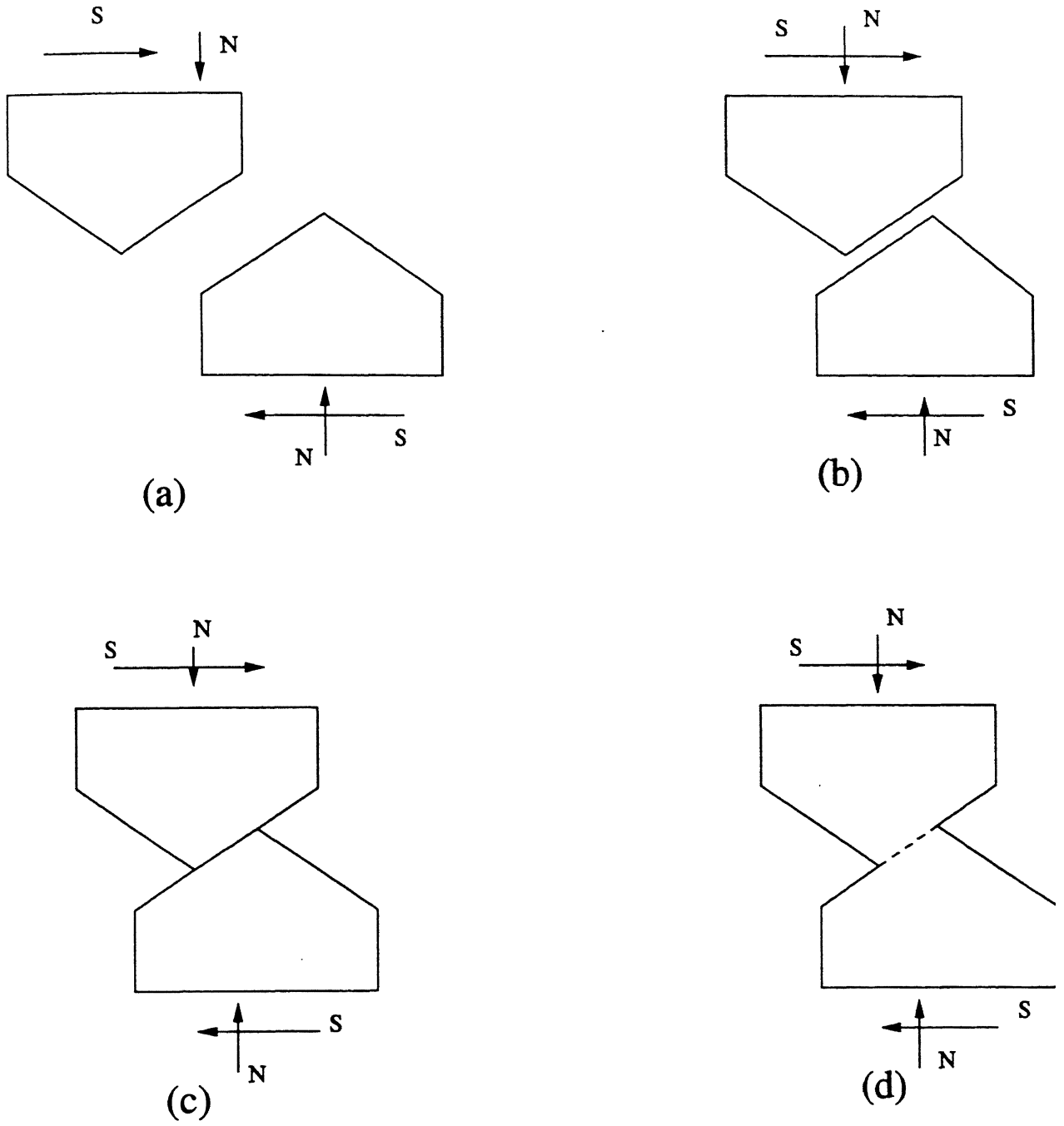

Figure 3.1: Junction Formation between two asperities.

From the various experiments [9,18], it can be concluded that two asperities of same or two different materials get welded during sliding and the junction gets the shape as shown in fig. 3.1(d). It was observed that junction tried to become symmetrical as a result of the load [9], as explained in fig. 1.7.

3.3 Experimental Description

The main aim of the experiments carried out was to view how the crack initiate and propagate inside a junction, formed because of adhesion of two asperities. The crack propagation was aimed to study as mainly qualitative. The experiments carried out were similar to those of Brockley and Tabour's experiments [18].

The experimental model had been taken as shown in fig. 3.2. The reason to take such model is explained in section 3.2. In real practice, the angle,θ may vary because of the normal load on the junction. Taking θ as one of the parameter, it was varied. This was to see the effect on the failure of the junction, if the asperities have different angles.

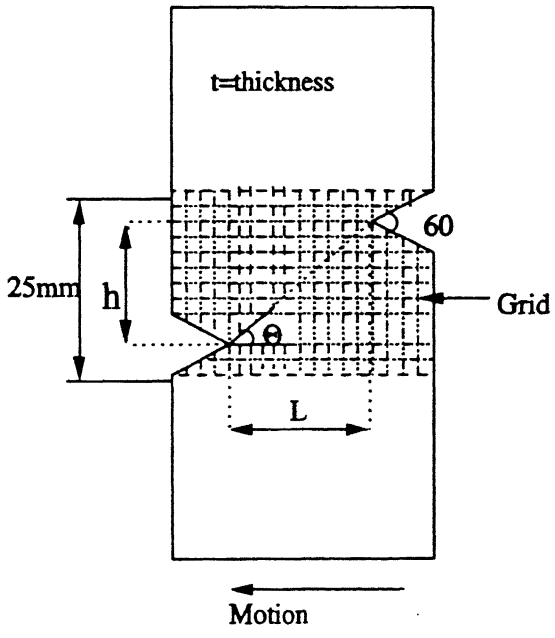

Figure 3.2: Specimen for Experiments.

The fixture for experimental work was made as shown in fig. 3.3. The guides were placed for perfect parallel motion between two halves of the fixture. The guides are fixed with the screws so that they can be removed if necessary. Taking into consideration that plate may topple from both sides while deformation takes place, arrangement was made with the help of two plates. These plates were fixed with the help of screws and can be removed while taking out the deformed plate.

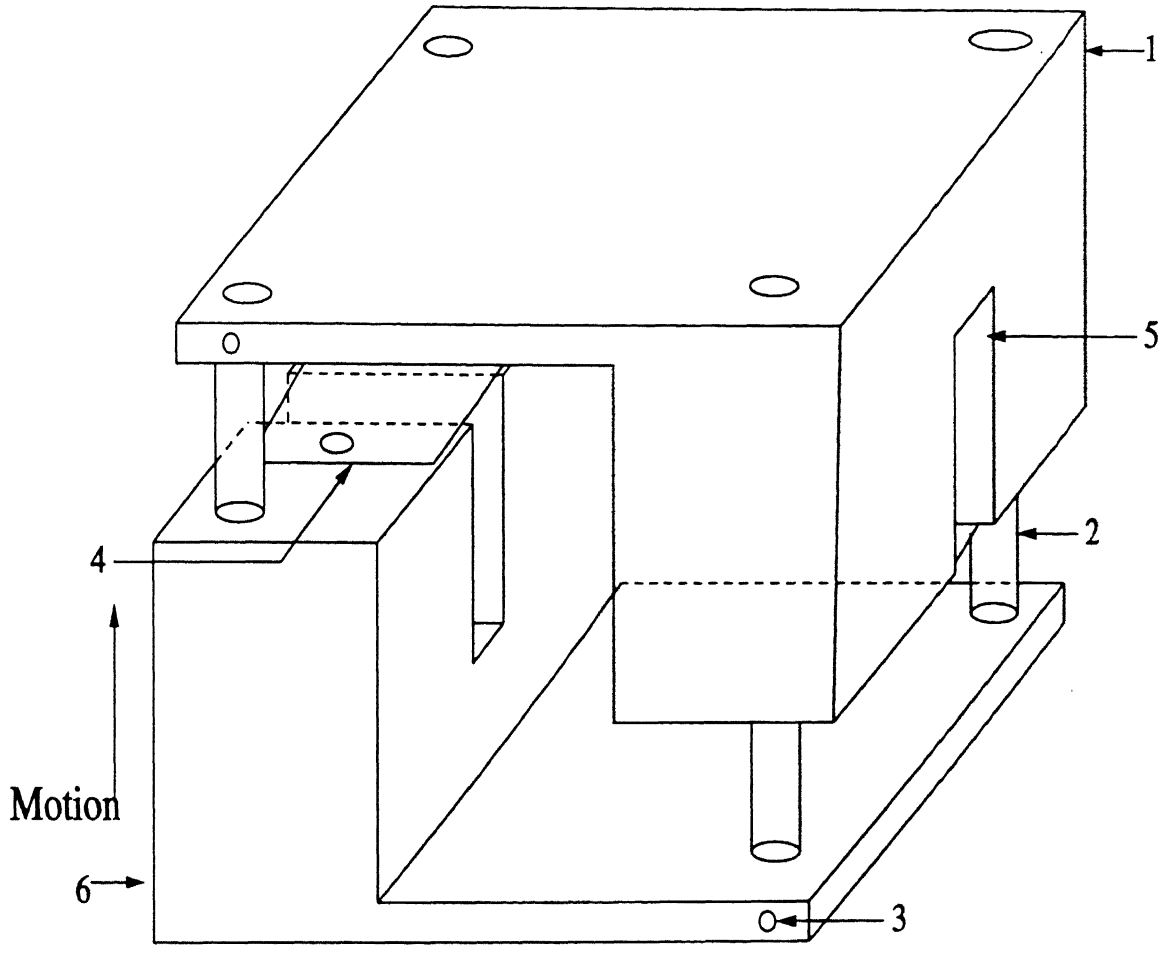

1.Upper half of the fixture
2. 4 guides for perfect parallel motion.
3. Screw for fixing the guide.
4. Plate to prevent toppling of the specimen.
5. Slot for the test specimen.
6. Lower half.

Figure 3.3: Fixture for Experiments.

The fixture was placed in a press. The experimental set-up is shown in fig. 3.4. The

bottom plate of press was moved upwards. Thus the one side of the plate was moving. and plate experienced only shear force.The pressure acting was measured with the help of a pressure gauge placed on the haudraualic cylinder which creates the pressure for the press. Test was stopped after the 20 mm travel of the platen of the press. The test piece was examined for the grid deformation and initiation of crack.

The materials used for experiments were

1. Lead
2. Copper
3. Mild Steel.

The thickness of the Lead and Copper specimen were 4.5 mm while that of Mild Steel was 3 mm.

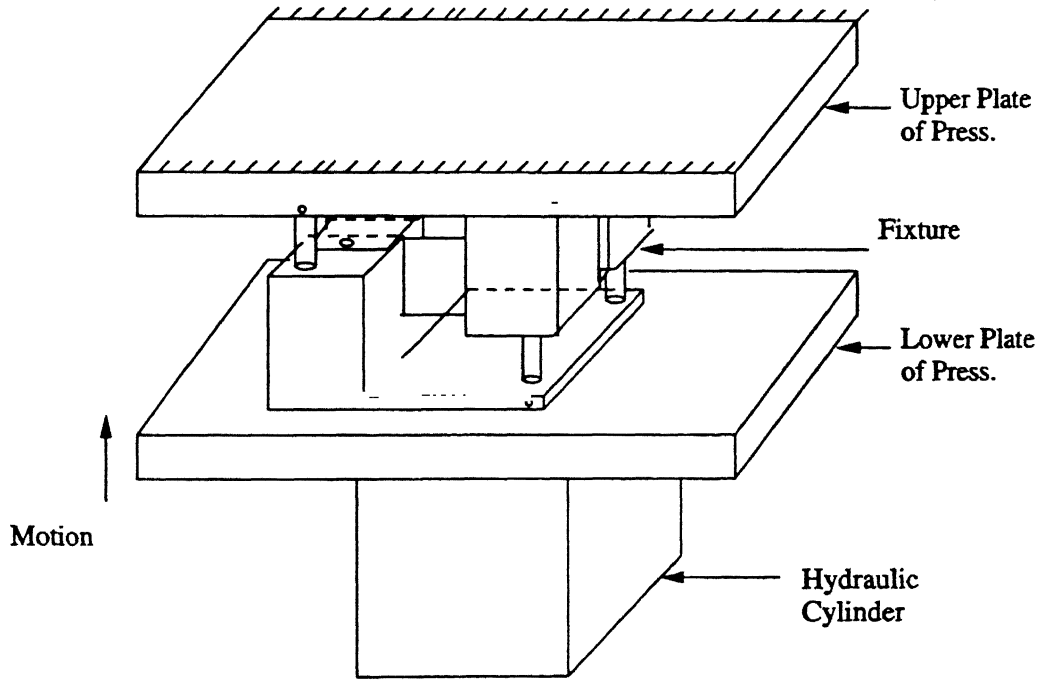

Figure 3.4: Experimental Set-Up.

The results are presented and discussed in section 4.1.

3.4 Calculation of Adhesion Wear Coefficient

The wear coefficient,K was calculated with the help of model explained by Brockley and Fleming [18].

In the present work two wear coefficients have been defined.

1)Adhesion Wear Coefficient, K.

2)Overall Wear Coefficient,Z.

The wear coefficient calculated from various experiments by various researchers is called as overall wear coefficient, Z. This Z is the number which reflects the probability that an encounter produces a wear particle. Z had been calculated from Archard's equation already explained in chapter one.

The wear coefficient calculated from FEM model is called as adhesion wear coefficient, K. This K is mere a number that reflects a parameter which in turn defines characteristic behavior of asperity fracture. It should be kept in mind that K is calculated from one asperity junction failure i.e. assuming encounter of only one asperity junction, while Z is a constant related to the probability that an encounter of asperities produces a wear particle and is estimated on the basis of interaction of a large number of asperity junctions of adhesive type and abrasion, diffusion also.

Adhesive wear is found to be governed by the Archard's wear equation [4],

$$V = \frac{ZlW}{P_m} \tag{3.1}$$

where,

V = Worn volume.

l = sliding distance.

W =applied load.

P_m = mean flow pressure.

Z = a constant related to the probability that an encounter will produce a wear particle.

Hirst [27] demonstrated that Z values are variable, but that the magnitude of this factor is usually small for 'actual' rubbing surfaces. Several laws of wear follows eq. 3.1.

1. The volume of worn material is proportional to sliding distance.
2. The volume of worn material is proportional to normal load.

Let's now consider the model shown in the fig. 3.5. It can be assume that the asperity junction have the same shape. Asperities I and II both are moving parallel to each other. The simulated load area can be taken as Lt., where L is the sliding distance for one asperity interaction and t is the thickness.

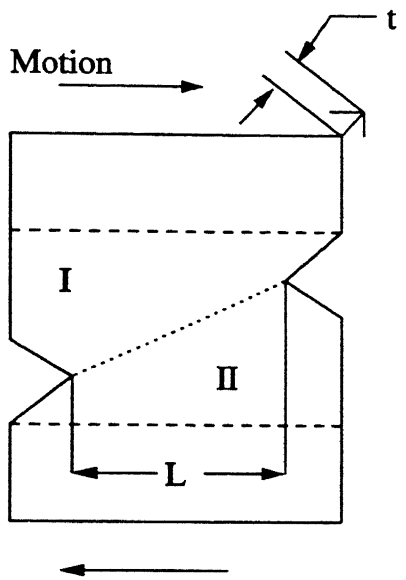

Figure 3.5: Model for Calculation of Wear Coefficient.

If it is assumed that the distance travelled during the formation of a particle is L, then

$$Wear\ Rate = R = \frac{V}{L} \tag{3.2}$$

Now P_m is the mean flow pressure and W is the normal load. This normal load is taken by the simulated area which is Lt. Therefore

$$Simulated\ Load\ Area = Lt = \frac{W}{P_m} \tag{3.3}$$

From previous three equations

$$K = \frac{R}{Lt} \tag{3.4}$$

$$K = \frac{V}{L^2 t} \tag{3.5}$$

This is the equation used for calculation for the wear coefficient.

The Wear Coefficients were plotted against the value of $\frac{E}{H}$. The Wear Coefficient, K was theoretical wear coefficient, i.e. it is based on the model assumed. The Wear Coefficient, Z is the wear coefficient calculated by various researchers [1,28]. This Z value is based on the wear debris, actually collected. This Z value have the effect of both adhesion and abrasion possibly diffusion also included. The value of K is calculated only taking into account of adhesion wear with some assumptions and is based on one asperity junction failure. Its definite aim of providing a loose particle and hence resulting in adhesive wear.

Chapter 4 shows the results of calculation of wear coefficient,K and shows the variation of K and Z vs $\frac{E}{H}$. The discussion is also carried out.

Chapter 4

Results and Discussions

This chapter presents experimental results and results based on finite element modeling, obtained for the fracture path of the welded asperity junctions. Broad discussion is also carried out.

4.1 Experimental Estimation of Adhesive Wear Coefficient

The experiments were carried out using three different materials,

1. Lead
2. Copper, and
3. Mild Steel.

Lead represents a perfectly plastic class of material, while Copper and Mild Steel represents a class of strain hardening materials.

The specimens were put in the fixture and sheared in the press. Fig. 3.4 shows a typical experimental setup and manner of load application. The results and discussion of the experiments are given below, where θ is the angle shown in fig. 3.2. Other variables are shown in the same figure.

The results of selected specimen are discussed below.

Test Specimen I :- Material-Lead

Specimen geometry: t=4.5 mm L=14mm θ=30^o.

The fig. 4.1 shows the photograph of first specimen. The specimen deformed and was found to be tending to be symmetrical in shape. The crack propagated before it becomes symmetrical. The cracks propagated well within the material, above and below the junction. The deformed grid showing clearly that junction was trying to become symmetrical. The plastic deformation had been seen at the tip of the cracks. That is showing that specimen would have broken for more displacement. The plate had been given the motion from one side only. This may be a reason for propagating the crack before junction becomes symmetrical.

Test Specimen II :- Material- Copper

Specimen geometry: t=4.5mm L=14mm θ=25^o.

The fig. 4.2 shows the photograph of second specimen. The junction has low value of θ than lead specimen. For higher value of θ, the junction could not break, as available motion was only 20 mm. The junction tried to become symmetrical, but not significantly. At the time of experiment, it had been examined that junction was trying to become symmetrical. The crack propagated into one asperity. In the other asperity the plastic deformation was seen at the tip of notch.

Test Specimen III :- Material- Mild Steel

Specimen geometry: t=3mm L=14mm θ=25^o.

The fig. 4.3 shows the photograph of third specimen. The specimen was trying to become symmetrical. The crack propagated in one asperity and on the verge of initiation in the other. Plastic deformation had been seen at the second notch. the value of θ is less for the same reason as that for copper.

Some kind of error came in the specimen, while the specimens were removing from the fixture. The specimens were bound to deform in reverse direction while removing them from the fixture. This error may give the feel that the junction were not trying to become symmetrical, but at the time of experiments the junction were more symmetrical than seen in the photographs.

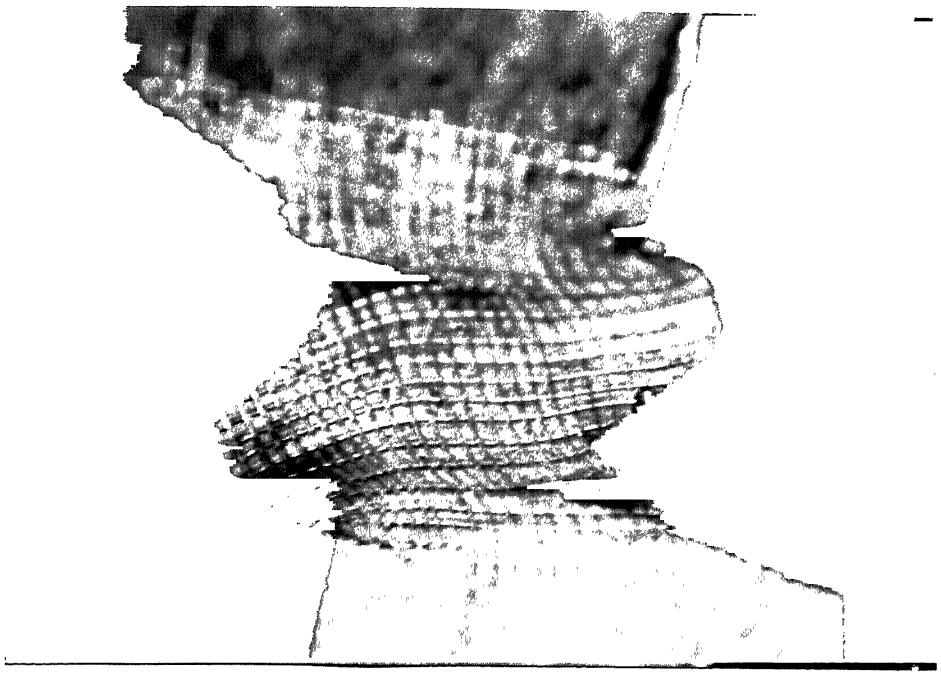

Figure 4.1: Photograph of Test Specimen I

Figure 4.2: Photograph of Test Specimen II

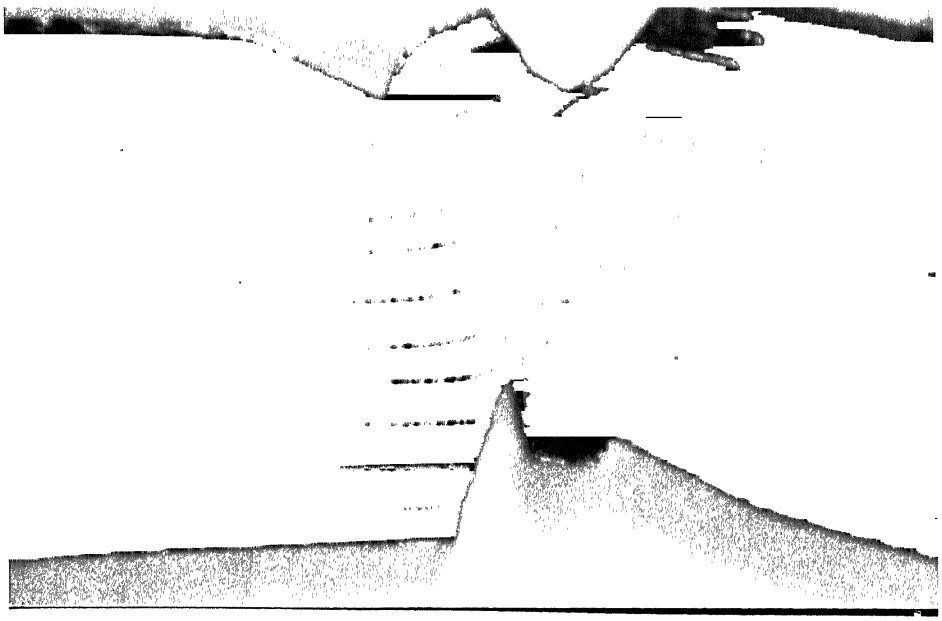

Figure 4.3: Photograph of Test Specimen III

The maximum distance by which the plate side could be moved was only 20 mm. This may be the reason for not propagating the crack for high value of θ. For high value of θ, the junction is too unsymmetrical and will require more displacement to shear. Only one side of the plate was moved, so there was no symmetrical deformation on both sides of the specimen and also crack initiated in one side first and then in other side.

Lead is more ductile than copper, but has less strength. So it broke even for high value of θ. Mild steel has more strength, but less ductile. So it didn't show large deformation.

The experimental results are not exactly matching with that one of Brockley and Fleming's [18]. The distance by which plate is moved is more in Brockley and Fleming's experiments compared to the present work.

Table 4.1 gives wear coefficient calculated using equation 3.5. The volume of wear is approximately calculated taking the rectangular area of the wear debris. The area was approximated as rectangular area as there was not sufficient crack propagation to assume to be circular area.

The wear coefficient for lead is highest, as it is softest material. Mild Steel has lowest wear coefficient, as it is tougher material than others. The wear coefficient of copper is

Material	Wear Coefficient, K
Lead-Lead	0.82
Copper-Copper	0.46
Mild Steel- Mild Steel	0.23

Table 4.1: Experimental Wear Coefficients (Eq. 3.5)

twice that of Mild Steel.

From the experiments it can be observed that when the junction is about to become symmetrical, the crack starts at the notch. This was prominently seen in lead test sample. Green [9] has also shown that, when junction becomes just symmetrical, the stress becomes tensile (fig. 1.7). The crack initiates because of this tensile stress. That means crack starts just before junction becomes symmetrical.

4.2 Finite Element Modeling Results

The crack path was found out for different materials as already explained in chapter 2.

The material combinations taken for the model were,

Unimetallic junction representation

1. Copper-Copper
2. Mild Steel-Mild Steel
3. Stainless Steel-Stainless Steel
4. Tungsten Carbide-Tungsten Carbide

Bimetallic junction representation

1.Mild Steel-Copper

2.Tungsten Carbide-Mild Steel

The properties of the materials are taken from various material reference books [29, 30, 31, 32].

Material	Copper	Mild Steel	Stainless St.	WC
Specific Weight, N/cc	0.0896	0.0785	0.0852	0.1930
Melting Point, ^oC	1083	1510	1083	2770
Elastic Modulus, N/mm^2	1.23×10^5	2.08×10^5	2.10×10^5	5.80×10^5
Modulus of Rigidity, N/mm^2	0.48×10^5	0.79×10^5	0.80×10^5	2.47×10^5
Thermal Conductivity, cal/s cm ^oC	0.940	0.120	0.121	0.75
Coeffi. of Linear Expansion, μm/m ^oC	16.2	11.1	10	5.2
Poisson's Ratio	0.26	0.3	0.3	0.17
Tensile Strength, MN/m^2	220	340	600	620
Hardness, BHN	40	137	170	900

Table 4.2: Properties of the materials.

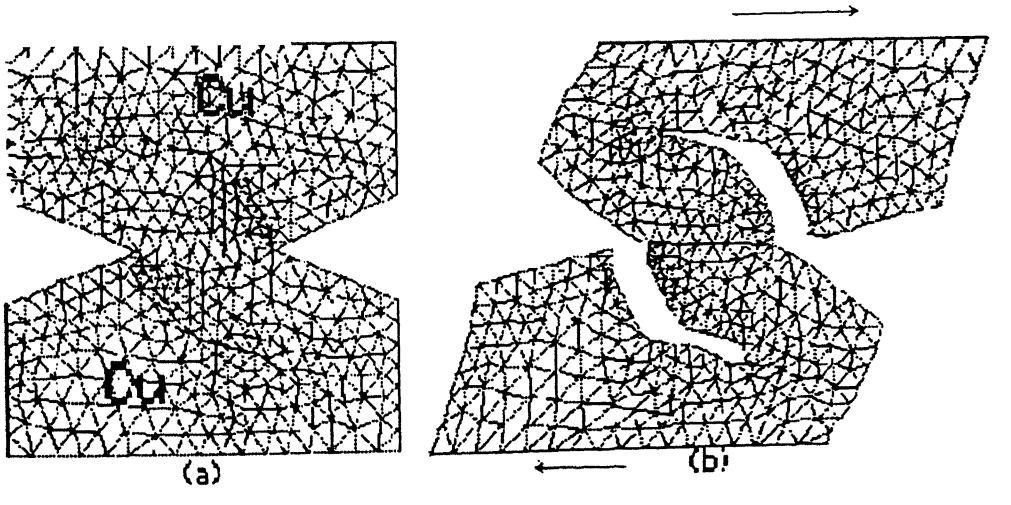

Figure 4.4: Copper/Copper (a) undeformed (b) deformed.

The figures show the fractured junctions.

Fig. 4.4 represents the copper/copper junction in undeformed and deformed state. One can see the crack propagated sufficiantly leading to fracture. The figure show qualitative agreement with that of the model experiment carried by Brockley and Fleming [18].

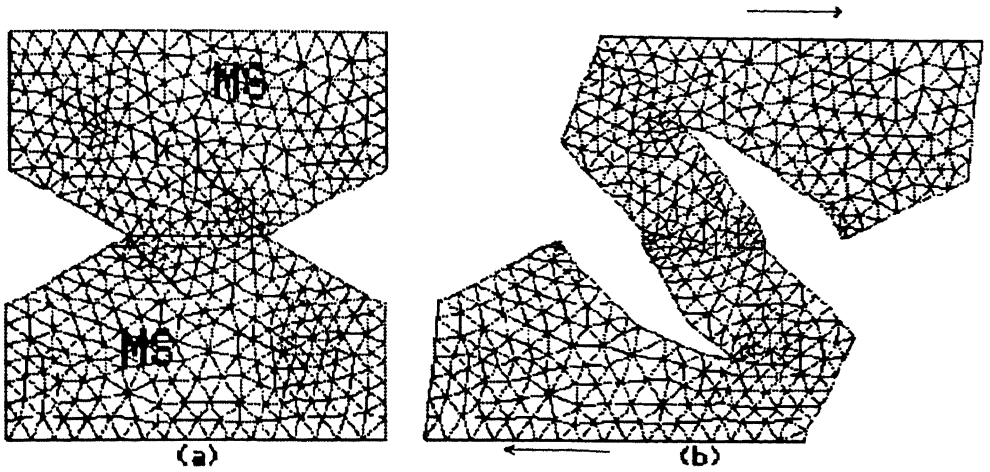

Figure 4.5: Mild Steel/Mild Steel (a) undeformed (b) deformed.

Fig. 4.5 represents mild steel/mild steel. The path is the qualitalivaly similar to that of copper, but nearer to the interface. This would indicate less loose wear material, eventually compares to wear material of Cu/Cu.

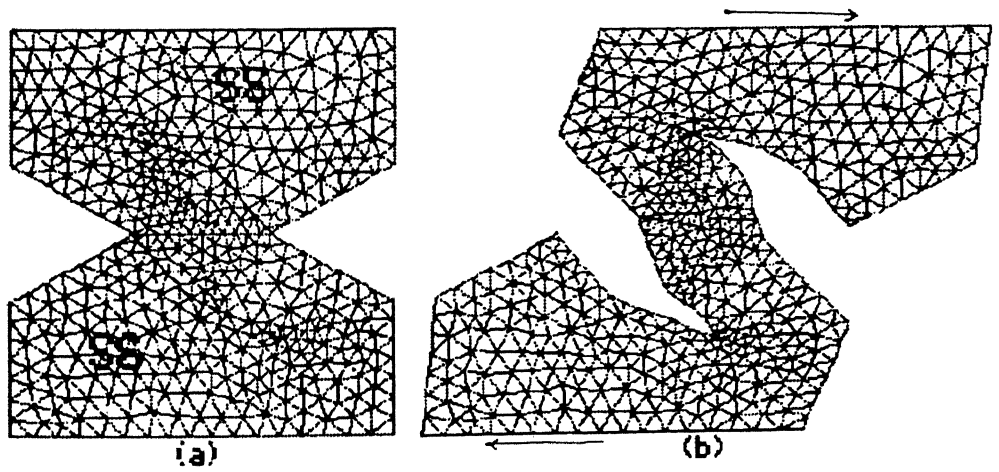

Figure 4.6: Stainless Steel/ Stainless Steel (a) undeformed (b)deformed.

Fig. 4.6 represents stainless steel/stainless steel junction. It is seen that the crack goes

in the similar manner, but the path is nearer to the interface if compared to Mild Steel and Copper.

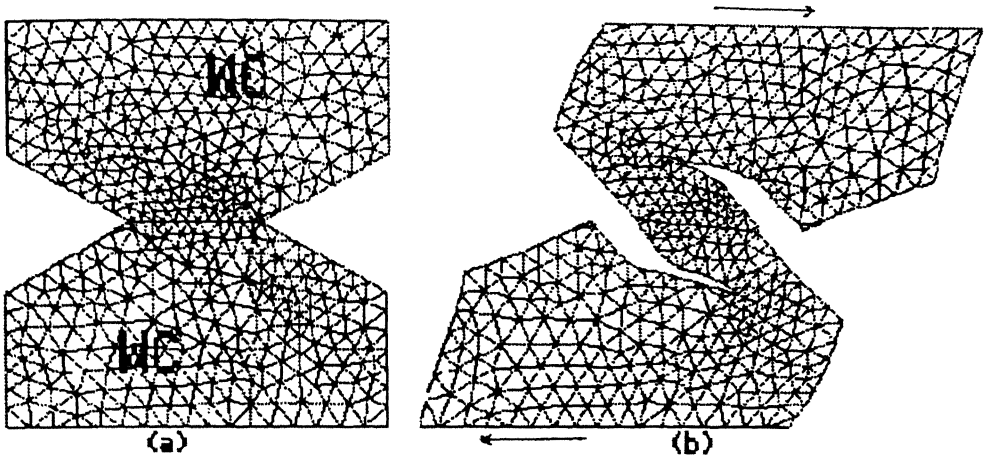

Figure 4.7: Tungsten Carbide/Tungsten Carbide (a) undeformed (b)deformed.

Fig. 4.7 represents tungsten carbide/tungsten carbide junction. The path is nearest to the interface.

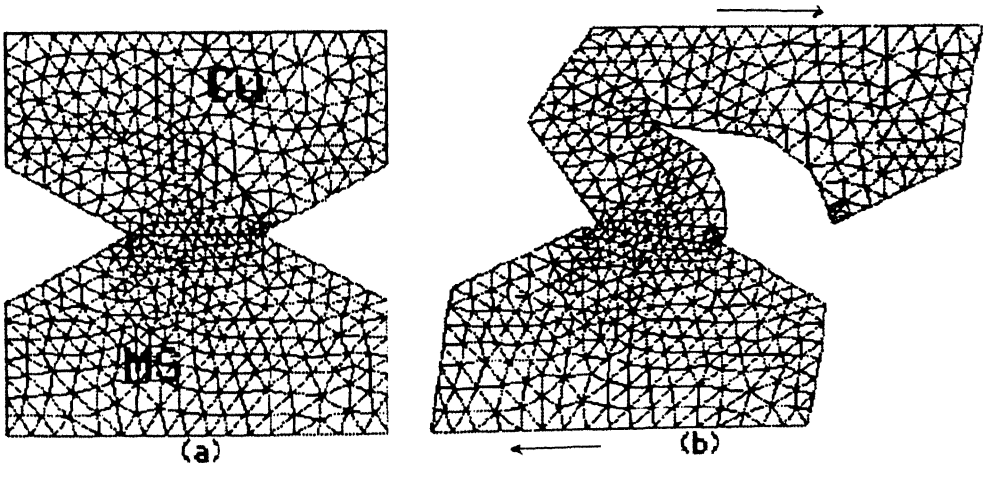

Figure 4.8: Copper/Mild Steel (a) undeformed (b) deformed.

Thus for unimetallic junction, the crack goes into both asperities. This is because of same strength of both the asperities.

The fig. 4.8 and fig. 4.9 shows copper/mild steel junction and mild steel/tungsten carbide junction respectively. The crack goes into the asperity of softer material, as the strength

of that material is less than the other and will fracture first.

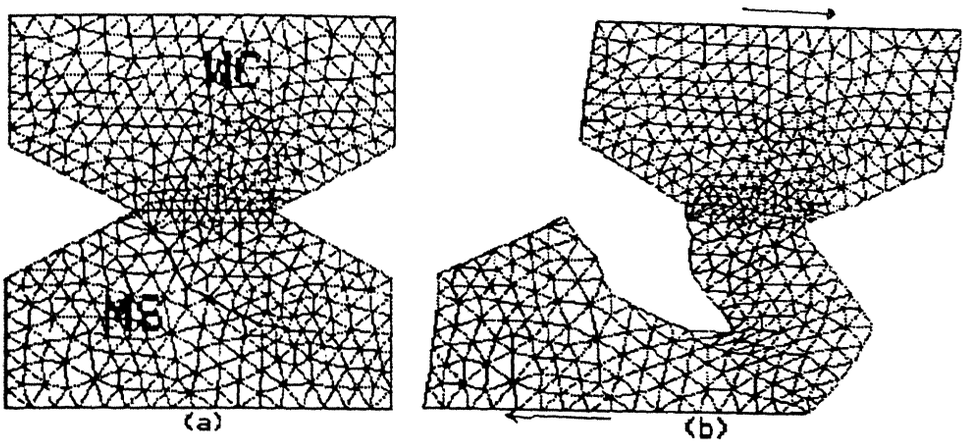

Figure 4.9: Model Mild Steel/Tungsten Carbide (a) undeformed (b) deformed.

The adhesion wear coefficient, K was calculated with the help of Eq. 3.5. Volume of wear was calculated by considering the area under the crack path and the thickness of test specimen.

In the present work, the wear coefficient calculated from FEM model is called as K. This K is mere a number that reflects a parameter which in turn defines characteristic behavior of asperity fracture. It should be kept in mind that K is calculated from one asperity junction failure i.e. assuming encounter of only one asperity junction.

Calculations of K for unimetallic and bimetallic asperity junctions as followed by Brockley and Fleming [18] are given in tables 4.3 4.4 respectively. The Brockley and Fleming's [18] calculation for Cu is also shown.

Materials (similar)	Wear Coefficient, K(FEM)*	Wear coefficient (Expt.)
Copper-Copper	2.0976	1.7 (Brockley)
Mild Steel-Mild Steel	1.1912	-
Stainless Steel-Stainless Steel	1.0451	-
Tungsten carbide-Tungsten carbide	0.6712	-

Table 4.3: Unimetallic Junction Results of K.

* represents present work.

Material (dissimilar)	Wear Coefficient, K(FEM)*	Wear coefficient (Expt.)
Mild Steel-Copper	0.645	-
Tungsten carbide-Mild Steel	0.6	-

Table 4.4: Bimetallic Junction Results of K.

The whole analysis was run on a Pentium processor and the time taken for that was approximately 45-50 minutes for an iteration. The complete analysis, the crack was propagated around 12-13 times, i.e. the iterations for one typical case. The time required for a typical case was around 10 hours.

4.3 Discussion on Results

The wear coefficient, Z estimated by various researchers using eq. 1.2 with the help of experiments by various researchers are given in tables4.5 and 4.6.

In the present work, the wear coefficient calculated from various experiments by various researchers is called as Z. This Z is the number which reflects the probability that an encounter produces a wear particle. Z had been calculated from Archard's equation already explained in chapter one. Z is a constant related to the probability that an encounter of asperities produces a wear particle and is estimated on the basis of interaction of a large number of asperity junctions of adhesive type and abrasion, diffusion also.

Materials (similar)	Wear coefficient, Z
Copper-Copper	32×10^{-3} [28]
Mild Steel-Mild Steel	7×10^{-3} [1]
Stainless Steel-Stainless Steel	21×10^{-3} [28]
Tungsten carbide-Tungsten carbide	1×10^{-6} [1]

Table 4.5: Values of Experimental Wear Coefficient, Z for unimetaliic Junctions.

Materials (similar)	Wear coefficient, Z
Mild Steel-Copper	1.5×10^{-3} [28]
Tungsten carbide-Mild Steel	4×10^{-6} [1]

Table 4.6: Values of Experimental Wear Coefficient, Z for Bimetallic Junctions.

On observing tables 4.3, 4.4, 4.5, 4.6 the first question arises in the mind is why K is much higher than that of Z. This is explained as follows.

In actual wear tests, a pin is made to rub against a rotating cylinder or a disc under a given load. The wear debris are collected after some time and the volume of the wear is calculated from weight loss. The wear coefficient calculations are done using this volume loss. In these tests the wear is not because of adhesion only. Wear is a very complex phenomenon. Other wear mechanisms such as abrasion, diffusion chemical action and fatigue are also working. For the calculation of K in the present work, these other mechanisms are neglected and only adhesion is considered as in Brockley and Fleming's work [18]. In the model it is assumed that two asperities have to get adhered, when they are brought together under load. This is not always true in practice. In actual rubbing it is not always true that each and every asperity get welded and then produces a wear particle. Also there may be thousands of encounters of asperities on the surface before loose wear debris become available. Also depending upon the relative mechanical and adhesion properties of two matching parts, the volume of wear debris will differ. The present adhesion model considers, each asperity encounter to yield one wear debri. In actual wear process wear debris are loose particle which may have gone back and forth between the bodies and large number of time takes ejecting out. It may also happen that broken part of one asperity adhere to the other asperity or get jammed in the valleys of two asperities. It has been actually observed that debris fill valleys [13]. In short, not every asperity takes part in the wear mechanism and give a loose particle. During actual rubbing of bodies the interaction and production of wear particles is a statistical phenomenon, while in the present model this nature of wear is totally ignored. The Z is defined in terms of probability because of above reason. As already mentioned in fig. 1.1, the wear coefficient of different processes in real situation is in range of 10^{-2}-10^{-8}, whereas K is not defined in terms of probability and so have much higher value than Z.

The two quantities Z and K do not have to be compared on the numerical values basis. How ever, materials of greater softness are expected to result in higher value of K, in the finite element model or actual asperity junction failure. Similarly as shown in fig 1.9, during actual rubbing, solid of higher compatibility would provide adhesive junction on a greater scale and hence should lead to higher values of Z compared to pairs having low compatibility. Fig 1.9 supports this agreement. As can be seen that R values has been shown to be greater for material with higher compatibility (open circles in fig. 1.9), higher R is also indicated for higher surface roughness and high coefficient of friction. Higher friction coefficient and higher surface roughness would naturally lead to the high adhesive wear and thus higher wear coefficient, Z and K as well. Therefore on a relative qualitative basis, it can be said that compatibility increases, wear coefficient increases.

Hence it is concluded that Z and K are expected to follow same trend . Figs. 4.10, 4.11 indeed show this behavior. It indicates that the finite modeling of asperity junction is fairly acceptable.

It can be seen that K for copper/copper from the finite element model agrees fairly well with that of Brockley's experimental model. There is not exact matching because in experiments, strain hardening takes place during deformation while it is ignored in the model. Strain hardening in practice would reduce value of wear coefficient, K.

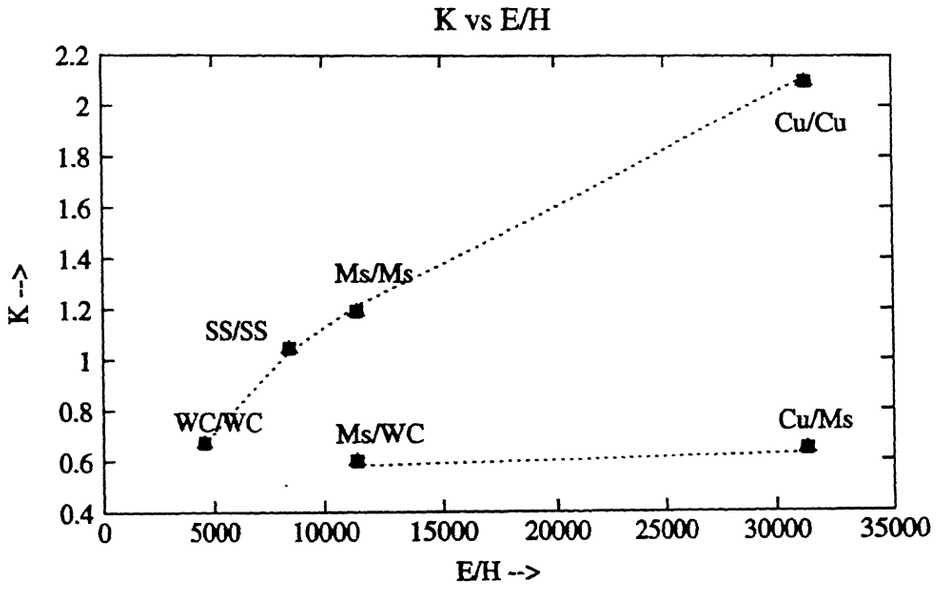

Figure 4.10: Variation of K against $\frac{E}{H}$.

Table 4.3 shows that the ratio of wear coefficients (FEM), K for Cu/Cu and MS/MS is almost two. This agrees with the ratio obtained on the basis of photographs (table 4.1). There is no exact matching of the wear coefficients as in model strain hardening due to deformation is neglected. It may be argued that because of strain hardening the wear tends to become low as material becomes hard.

It can be seen from the results that the metals having greater compatibility have higher wear coefficient which in turn result in more wear. It is also seen that bimetallic junctions have less wear coefficient than unimetallic junction. It fairly agrees with the experimental work.

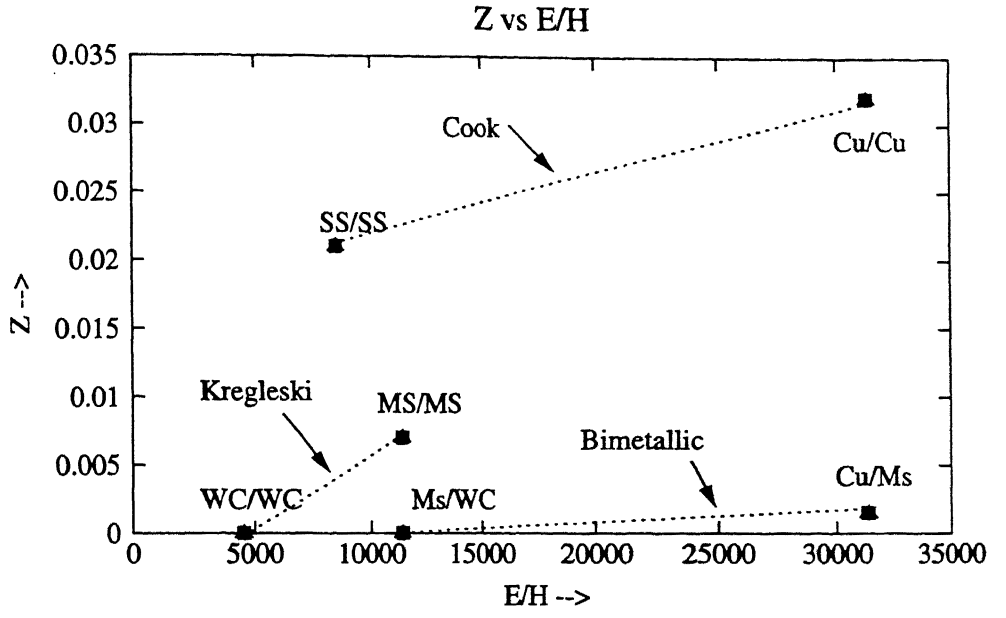

Figure 4.11: Variation of Z against $\frac{E}{H}$.

As already mentioned in section 1.1.4, the wear coefficient depends on the ratio of $\frac{E}{H}$. In the present work also an attempt is made to corelate the ratio of $\frac{E}{H}$ with wear coefficient, K. The plot of K vs $\frac{E}{H}$ is shown in fig. 4.10. It can be observed from the figure that as $\frac{E}{H}$ increases, K increases. The unimetaliic junctions show a slope and which differs from that of bimetallic junctions. It shows that two cases are best studied separately. Bimetallic Junctions have less wear coefficient compared to the unimetaliic junctions. If bimetallic junction have lesser value of R, compared to unimetallic junction then their adhesion wear coefficient would be lesser. Fig. 4.11 gives the variation of the Z against $\frac{E}{H}$. This graph agrees with that of the model and gives the similar trend of the wear coefficient. The values of Z for SS and Cu are taken from Cook [28] and that for MS and WC are taken from Kregleski [1]. The experiments carried out by these two researchers are not under identical conditions and so the values should be placed in different groups. The values of Z for different metals are taken from these two references and have much lower value compares to Z value for similar metal experiments. This graph of Z (fig. 4.11) agrees with graph of K (fig. 4.10) and gives the similar trend of the wear coefficient.

Fig. 4.12 shows the graph of K vs $\frac{E}{H}$ for some selected materials which have lower value of K and Z. This is the zooming of the fig. 4.10 at the lower range. This graph is shown for giving better idea of the wear coefficients having low value. Similarly Fig. 4.13 gives the variation of Z against $\frac{E}{H}$ for same materials. It can be argued that these metals fall

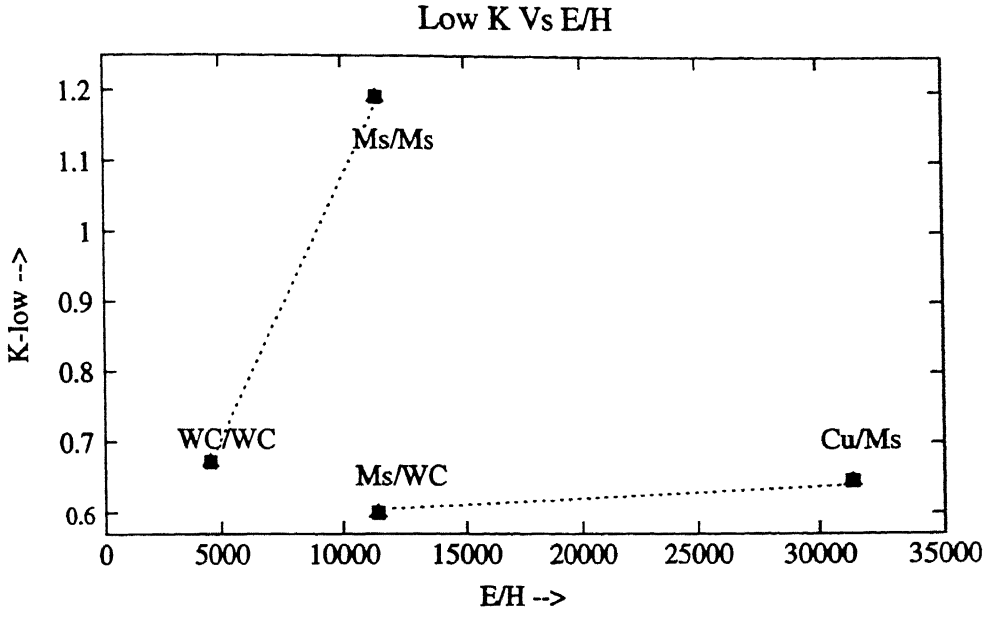

Figure 4.12: Variation of K against $\frac{E}{H}$ for materials having low K

in one category of having less hardness.

It can be seen from all graphs that for metals having high compatibility, wear coefficient is high and for low compatibility metals, wear coefficient is low. For unimetallic junctions, compatibility is high and for bimetallic junctions compatibility is low, so generally unimetallic junctions have higher value of wear coefficient than bimetallic junctions. Cu/MS has high compatibility compared to WC/MS, so wear coefficient, K for Cu/MS is higher than that for MS/WC. Rabinowicz [23] also showed that for high compatibility metals, wear coefficient is more (fig. 1.9). There may be some discrepancies as wear is a very complex phenomenon and can't be defined by adhesion only.

Bimetallic wear coefficient is also plotted in above graphs. These bimetallic form next category. Bimetallic junctions have less wear than those of unimetallic. This is acceptable as for bimetallic junction, only one asperity is prone to loose material.

The fig. 4.12 and tables 4.5 and 4.6 show that K for WC/MS is less than K for WC/WC while Z for WC/MS is higher than Z for WC/WC. As explained earlier, several wear mechanisms along with adhesion mechanism may simultaneously working. While experiments are carried out by researchers on mild steel with tungsten carbide, mild steel is bound to get abrade because of tungsten carbide's high hardness compared to mild steel.

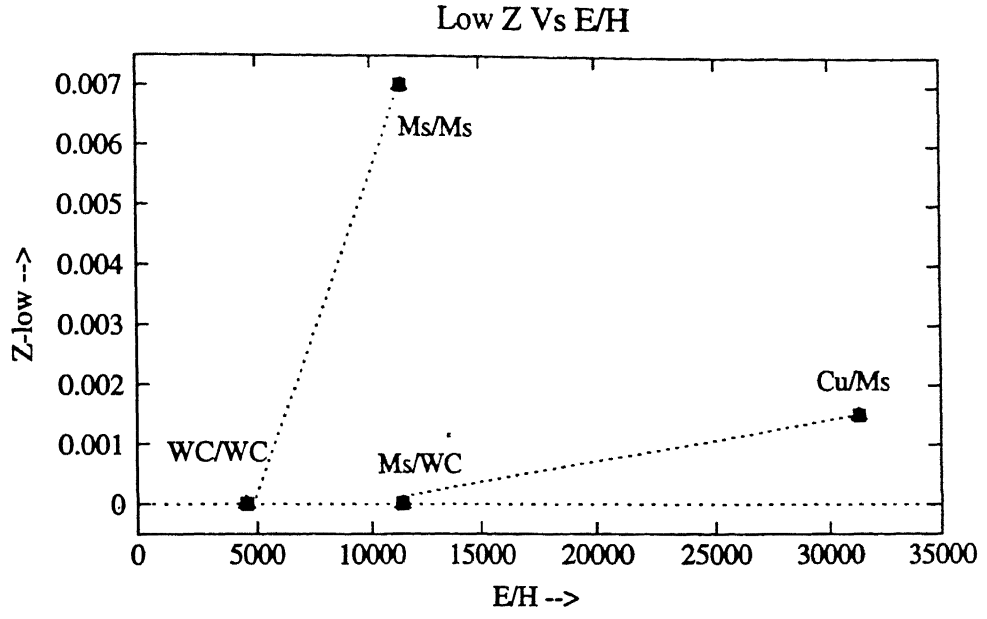

Figure 4.13: Variation of Z against $\frac{E}{H}$ of metals having low Z

Also mild steel and tungsten carbide have less compatibility, so there is less chance of adhesion between the asperities of both metals, in turn less adhesive wear. Because of all these reasons the experimental wear coefficient, Z of WC/MS is more than that of WC/WC.

Material	$\frac{Z}{K} \times 10^{-3}$	Compatibility
Copper-Copper	11	High
Mild Steel-Mild Steel	6	Medium
Copper-Mild Steel	2.3	Low
Mild Steel-Tungsten Carbide	0.006	Very Low

Table 4.7: Variation of $\frac{Z}{K}$ vs Compatibility.

An attempt has been made to relate the K with Z. It may be useful in future if one get a fairly acceptable relation between K and Z to predict wear coefficient for other materials. Table 4.7 shows the ratio of Z and K for selected metals depending on their compatibility. It can be observed that as compatibility decreases the ratio decreases. The similar trend is observed as that observed by Rabinowicz [22], for low compatibility wear coefficient, Z is low.

Chapter 5 gives conclusion and suggetions for future scope

Chapter 5

Conclusion and Suggestions for Future Scope

5.1 Conclusion

1. The path of fracture gives qualitative agreement to the experiment done by Brockley and Fleming.

2. Experiments show that the crack goes into both asperities.

3. Adhesive wear coefficient is higher for unimetallic junctions than for bimetallic junctions. This shows that for higher compatibility metals, wear coefficient is more, in turn more wear.

4. Wear coefficient increases as the ratio of Elastic modulus to the Hardness of a softer material in the junction increases. The adhesive wear coefficient gives similar trend to the wear coefficient (defined using Archard's equation) when plotted against ratio of Elastic modulus to Hardness of a softer material in the junction.

5. Present model gives qualitative trend of the wear coefficient, which is important for the cases of bearing materials or cutting tools.

The work is however far from complete and the model may need to be examined in some detail as outlined below.

5.2 Suggestions for Future Scope

1. In future one should try to accommodate statistical data of asperity size distribution.
2. The present analysis allows crack to propagate along the edges of elements only. More realistic analysis can be modelled by propagating the crack across the elements also.
3. Plastic analysis with large deformation theory may give better results.
4. Consideration of strain hardening during the deformation of the junction may yield to good results.

Bibliography

[1] Kregleski, I. V.,"Friction and Wear", Butterworths, Washington (1965).

[2] Sarkar, A. D.,"Wear of Metals", Pergamon Press, 1976.

[3] Holm, R.,"Electrical Contacts", Stockholm, Gerbers (1946).

[4] Archad, J. F.,"Contact and Rubbing of Flat Surfaces", Jr. Appl. Phys., 24 (1953) 981.

[5] Rabinowicz, E., "the Least Wear", Wear, 100 (1984) 533.

[6] Green, A. P.,"The Plastic Yielding of Metal Junctions due to combined Shear and Pressure", Jr. Mech. Phys. Solids, 2 (1954) 197.

[7] Muju, M. K.,"Effect of Magnetic Field on Wear", Ph. D. Thesis, 1975.

[8] Bowden, F. P. and Tabor, D.,"The Friction and Lubrication of Solids", Clarendon Press, Oxford (1954).

[9] Green, A. P.,"Friction between Unlubricated Metals, A Theoretical Analysis of the Junction Mode", Proc. of Roy. Soc. (London), 228C (1955) 191.

[10] Edward, C. M. and Halling, J., "An Analsis of the Plastic Interaction of Surface Asperities and its relevance to the Coefficient of Friction", Mech. Engg. Sci., 10 (1968).

[11] Gupta, P. K. and Cook, N. H.,"Junction Deformation Models for Asperities in Sliding Interaction", Wear, 20 (1972) 73.

[12] Ling, F. F. and Pan, C. H. T.,"Approaches to Modelling of Friction and Wear", Springer-Verlag, 1986.

[13] Sreenath, A. V. and Raman, N.,"Mechanism of smoothning of cylinder liner surface during running -in", Tribol. Int., 9 (1976) 55.

[14] Buckley, D. H., Cobalt, 38 (1968) 20.

[15] Stott, G. and Eyre, J.,"A Practical Interpretetion of Unlubricated Wear data for some Non-Ferrous Metals", Wear, 50 (1978) 285.

[16] Karamis, M. B. and Odabas, D.,"A Simple Approach to Calculation of Sliding Wear Coefficient for Medium Carbon Steels", Wear, 151 (1991) 23.

[17] Kerridge, M. and Lancaster, J. K., Proc. Roy. Soc., A236 (1956) 250.

[18] Brockley, C. A. and Fleming, G. R.,"A Model Junction Study of Serve Metallic Wear", Wear, 8 (1965) 374.

[19] Baliga, V.,"An Application of FEM to the Study of Asperity Junctions in Adhesive Wear", M. Tech. Thesis., 1986.

[20] Roach, A. F., Goodzeit, C. L. and Totta, P. A., Nature, 172 (1953) 301.

[21] Roach, A. F., Goodzeit, C. L. and Hunnicatt, R. P., Trans. American Soc. Mech. Engrs., 78 (1956) 1659.

[22] Rabinowicz, E., "The Dependance of the Adhesive Wear Coefficient on the Surface Energy of the Adhesion", The International Conference on Wear of Materials, Missouri, (1977) 36.

[23] Rabinowicz, E., "Infuence of Surface Energy on Friction and Wear Phenomenon", Jur. Appl. Phys., 32 (1961) 1440.

[24] Halling, J. and El-refaie, M., Tribology Convection, Inst. Mech. Engrs., (1971), 60.

[25] Reddy, J. N.,"An Introduction to the Finite Element Method", McGraw-Hill, Inc., 1993.

[26] Zienkiewicz, O. C., "The Finite Element Method", McGraw Hill Book Company, London, 1977.

[27] Hirst, W., Proceedings of the Conference on Lubrication and Wear, Institution of Mechanical Engineers, London, 674.

[28] Cook, N. H.,"Manufacturing Analysis", Addison Wesley Publications, 1966.

[29] Smithells, C. J.,"METALS, Reference Book", Vol. II, Butterworths, London, 1967.

[30] PSG Design Data Book

[31] Young, J. F.,"Materials and Processes", John Willy and Sons, Inc., Newyork, 1953.

[32] Westermann Tables, for The Metal Trade, Edited by Hermann Jujz and Edward Schartus, Willy Eastern Ltd., New Delhi, 1966.